AD_____

Award Number: W81XWH-08-1-0394

TITLE: Interplay of CREB and ATF2 in Ionizing Radiation-Induced Neuroendocrine Differentiation of Prostate Cancer Cells

PRINCIPAL INVESTIGATOR: Chang-Deng Hu

CONTRACTING ORGANIZATION: Purdue University
West Lafayette, IN 47907

REPORT DATE: June 2011

TYPE OF REPORT: Annual

PREPARED FOR: U.S. Army Medical Research and Materiel Command
Fort Detrick, Maryland 21702-5012

REPORT DOCUMENTATION PAGE

Form Approved
OMB No. 0704-0188

1. REPORT DATE *(DD-MM-YYYY)*	2. REPORT TYPE	3. DATES COVERED *(From - To)*
01-06-2011	Annual	1 JUN 2010 - 31 MAY 2011

4. TITLE AND SUBTITLE

Interplay of CREB and ATF2 in Ionizing Radiation-Induced Neuroendocrine Differentiation of Prostate Cancer Cells

5a. CONTRACT NUMBER

5b. GRANT NUMBER
W81XWH-08-1-0394

5c. PROGRAM ELEMENT NUMBER

6. AUTHOR(S)
Chang-Deng Hu

E-Mail: hu1@purdue.edu

5d. PROJECT NUMBER

5e. TASK NUMBER

5f. WORK UNIT NUMBER

7. PERFORMING ORGANIZATION NAME(S) AND ADDRESS(ES)
Purdue University
West Lafayette, IN 47907

8. PERFORMING ORGANIZATION REPORT NUMBER

9. SPONSORING / MONITORING AGENCY NAME(S) AND ADDRESS(ES)
U.S. Army Medical Research and Materiel Command
Fort Detrick, Maryland 21702-5012

10. SPONSOR/MONITOR'S ACRONYM(S)

11. SPONSOR/MONITOR'S REPORT NUMBER(S)

12. DISTRIBUTION / AVAILABILITY STATEMENT
Approved for Public Release; Distribution Unlimited

13. SUPPLEMENTARY NOTES

14. ABSTRACT

Radiation therapy is a first line treatment for prostate cancer patients and the patient's response is generally good. However, approximately 10% of low-risk and up to 60% of high-risk prostate cancer patients will experience biochemical recurrence within five years after radiotherapy. We have found that following a clinical radiation therapy protocol (2 Gy/day, 5 days/week), ionizing radiation (IR) induced the LNCaP prostate cancer cells to transdifferentiate into neuroendocrine-like (NE-like) cells, a process also known as neuroendocrine differentiation (NED) that is associated with disease progression and the acquisition of androgen-independent growth. Once differentiated, the NE-like cells are highly resistant to radiation and survive the treatment without any obvious cell death. Furthermore, we have demonstrated that two transcription factors, CREB and ATF2 oppose each other to regulate IR-induced NED. Further evidence suggests that ATF2 acts as a transcriptional repressor and CREB functions as a transcriptional activator in NED. Significantly, we also found that IR-induced NE-like cells are reversible and dedifferentiated cells are cross-resistant to radiation, androgen ablation and chemotherapeutic agent docetaxel treatments. We have also extended our findings in LNCaP cells to three other prostate cancer cell lines and demonstrated that IR also induced NED in xenograft nude mouse models. These findings suggest that radiation-induced NED may represent a novel pathway by which prostate cancer cells survive the treatment and contribute to recurrence.

15. SUBJECT TERMS
LNCaP, prostate cancer, ionizing radiation, neuroendocrine differentiation, ATF2, CREB

16. SECURITY CLASSIFICATION OF:			17. LIMITATION OF ABSTRACT	18. NUMBER OF PAGES	19a. NAME OF RESPONSIBLE PERSON
a. REPORT	b. ABSTRACT	c. THIS PAGE			USAMRMC
U	U	U	UU	69	19b. TELEPHONE NUMBER *(include area code)*

Table of Contents

Introduction

The neuroendocrine (NE) cells are one of the three types of epithelial cells in the human prostate, and are present in almost all cases of prostatic adenocarcinoma [1, 2]. Although the physiological role of NE cells in the normal prostate remains unclear, increased number of NE-like cells is found in advanced prostate cancer. Accumulated evidence suggests that NE-like cells produce a number of growth factors or peptide hormones that facilitate the growth of surrounding tumor cells in a paracrine manner, and that NE-like cells are clinically associated with androgen-independent growth of prostate cancer [1-4]. Consistent with this, androgen ablation can also induce NE differentiation (NED) of prostate cancer *in vitro* and *in vivo* [4-10]. Hence, the number of NE-like cells appears to be an indicator of prostate cancer progression. In addition to androgen ablation, IL-6 [11-16] and agents that can elevate the intracellular levels of cAMP [12, 17-20] also induce NED. Recently, our preliminary results showed that ionizing radiation (IR) also induced NED *in vitro*. Interestingly, we observed that irradiated cells showed increased cytoplasmic localization of activating transcription factor 2 (ATF2) and an increase in the phosphorylated form of cAMP response element binding (CREB) protein. Since ATF2 and CREB both belong to the basic region leucine zipper (bZIP) family of transcription factors and bind the same cAMP response element (CRE) as a homodimer or a heterodimer to regulate gene transcription [21]. While some target genes can be activated by CREB and ATF2 equally or cooperatively [22-24], differential regulation of other target genes by CREB and ATF2 has also been observed [25-29]. Importantly, CREB is implicated in prostate cancer growth [30], acquisition of androgen independent growth [31], cAMP-induced NED [18, 32], and transcription of prostate-specific antigen [33]. Based on these preliminary findings, we proposed that ATF2 may function as a transcriptional repressor and CREB acts as a transcription activator of NED. Hence, IR induces NED by sequestering ATF2 in the cytoplasm and activating CREB in the nucleus. To determine how ATF2 and CREB regulate NED at the transcriptional level, we proposed three specific aims in the applications: **(1)** determine functional relationship between CREB and ATF2 in IR-induced NED; (**2**) elucidate molecular mechanisms underlying regulation of IR-induced NED by pCREB and ATF2; **(3)** identify cytoplasmic signals responsible for the cytoplasmic sequestration of ATF2 and nuclear accumulation of pCREB. Given that NE-like cell is an indicator of cancer progression and that NE-like cells are highly resistant to radiation- and other agents-induced apoptosis, our novel observation that IR can induce NED of prostate cancer cells uncovers a novel pathway by which tumor cells may develop radioresistance. Successful completion of this project will allow for the development of novel radiosensitization approaches by targeting NED at the transcriptional regulation level.

Body

Completion of Approved Statement of Work

Task 1. Aim 1: Determine the functional relationship between CREB and ATF2 in IR-induced NED (Months 1-18)

a. We will first use LNCaP cells to establish stable cell lines expressing tetracycline repressor (Months 1-3)
b. Subclone our current two siRNA constructs for both CREB and ATF2 into pRNATin-H1.2/Neo vector and stably transfect them into repressor-expressing cell lines to isolate stably integrated clones (Months 2-6).
c. Subclone cDNAs encoding different CREB and ATF2 mutants into pcDNA4/TO vector (Months 4-6).
d. Establish stable cell lines expressing siRNA and different mutant CREB and ATF2 proteins (Months 6-12).
e. Optimize expression conditions (Months 7-10).
f. Examine knockdown effect of CREB and ATF2 on IR-induced NED (Months 7-18).
g. Examine the effect of overexpressed constitutively cytoplasmic- and nuclear-localized pCREB or ATF2 on IR-induced NED (Months 7-18).

We have successfully used LNCaP cells to establish several stable cell lines expressing tetracycline repressor. Screening of these stable cell lines identified one that showed high expression of the tetracycline repressor. This cell line was also used to establish several stable cell lines [pcDNA4/TO, pcDNA4/TO-CREB(S133A), pcDNA4/TO-nATF2, pRNATin-H1.2/Neo-ATF2shRNA, pRNATin-H1.2/Neo-CREBshRNA)]. Three stable cell lines expressing the dominant negative mutant CREB (CREB-S133A) and the constitutively nuclear-localized ATF2 (nATF) were used to assess their role in IR-induced NED. We found that induction of CREB-S133A or nATF2 inhibited IR-induced NED. The results have been presented in our Cancer Research paper [34]. Results are presented in Figure 4 (page 9667) and methods are presented on page 9664.

We have also demonstrated that overexpression of a constitutively cytoplasmic-localized ATF2 induced NED. This is due to the sequestration of endogenous ATF2 in the cytoplasm by cATF2. This result is similar to NED induced by ATF2 knockdown in transient transfection. These results are presented in Figure 3 (page 9666) and Supplemental Figures 2 and 3.

We failed to obtain the induction of shRNAs in several stable lines during the first year and we continued the screening and identified several clones that can express shRNA to knockdown CREB. Since CREB-S133A failed to inhibit IR-induced CgA and NSE expression, we put more effort to determine the critical role of CREB in IR-induced NED. Because CREB can be phosphorylated and activated by multiple phosphorylation at multiple sites [35], we reasoned that targeting of CREB using knockdown or other dominant negative mutants would allow elucidation of the critical role of CREB in IR-induced NED. For this purpose, we continued to search for other stable cell line clones

that allow for inducible knockdown of CREB and we have identified one. In addition, we have also established several cell lines to express two other types of dominant negative mutants of CREB: A-CREB and bCREB. A-CREB has been successfully used to target CREB [36, 37] and bCREB is the bZIP domain only without any transactivation domain. With these materials in hands, we have demonstrated that targeting of CREB by overexpressed A-CREB sensitized LNCaP cells to IR (Fig. 1). We are currently looking at possible mechanisms. We have also used the inducible CREB knockdown clones to demonstrate that inhibition of CREB by itself is sufficient to inhibit IR-induced NED (Fig. 2).

Task 2. Aim 2: Elucidate molecular mechanisms underlying the promotion of NED by pCREB and the repression by ATF2 (Months 12-24)

a. Make reporter gene constructs or obtain from other labs and optimize ChIP conditions (Months 12-16).
b. Determine the effect of pCREB and ATF2 on CgA-Luc activation (Months 12-16).
c. Perform ChIP assays to determine the kinetic changes in the binding of pCREB, CREB, ATF2 and other possible AP-1 proteins on the CRE site in the CgA promoter and NSE promoter in response to IR (Months 16-24).
d. Determine the role of ATF2 in prostate cell growth and cell death (Months 16-24).

We have successfully completed all of the proposed experiments. (1) We performed EMSA assays and confirmed that CREB and ATF2 both can bind the conserved CRE site in the CgA promoter (Fig. 3). (2)We made CgA and NSE luciferase reporter gene constructs and examined the effect of CREB and ATF2 on these reporter genes. We indeed observed that IR can activate the CgA reporter gene and its activity can be inhibited by ATF2 (Fig. 4). (3) We also performed ChIP assay and found that IR increased pCREB binding to the CgA promoter (Fig. 5). However, the binding of ATF2 to the CgA promoter did not change in non-irradiated or irradiated cells. (4) We observed that knockdown of ATF2 also induced neurite extension and cell death. Some of these results were already published in the Cancer Research paper [34].

Task 3. Aim 3: Determine how IR induces cytoplasmic sequestration of ATF2 and identify cytoplasmic signals that may regulate subcellular localization of pCREB and ATF2 (Months 24-36)

a. Examine whether IR increases ATF2 homodimerization in the cytoplasm (Months 24-28).
b. Examine whether IR stabilizes the intramolecular interaction of ATF2 (Months 24- 28).
c. Examine the effect of AKT on the subcellular localizations of ATF2 and pCREB (Months 24-36).
d. Screen for other possible cytoplasmic signal that may be involved in regulating the subcellular localizations of ATF2 and pCREB (Months 24-36).
e. Identify cytoplasmic interacting proteins of pCREB and ATF2 using mass

spectrometry and functionally determine the roles of candidate interacting proteins in regulating the subcellular localizations of pCREB and ATF2 and in regulating IR-induced NED (Months 24-36)

We have screened several other protein kinases including AKT using specific inhibitors to determine whether any of these protein kinases might be involved in radiation-induced CREB phosphorylation. We identified PKA as a potential protein kinase responsible for IR-induced CREB phosphorylation during the first week treatment (Fig. 6). We have also initiated our collaboration with Dr. Andy Tao to identify cytoplasmic interacting proteins of ATF2 and CREB. We have identified some candidate proteins and we demonstrated that CaMKII as a cytoplasmic interacting protein of pCREB (Fig. 7). We also found that IR increased nuclear localization of CaMKII (Fig. 8). However, inhibition of CaMKII activity by its specific inhibitor KN-93 did result in any reproducible results.

Additional accomplishments beyond the Approved SOW

(1) We have also demonstrated that IR-induced NED is reversible. Importantly, we have isolated three dedifferentiated clones and found that these dedifferentiated cells have acquired the ability to be cross-resistant to radiation, androgen ablation, and chemotherapeutic agent docetaxel. Also, these dedifferentiated clones respond poorly to IR- or androgen ablation-induced NED. These findings strongly suggest that IR-induced NED may represent a novel pathway by which prostate cancer cells survive the treatment and contribute to recurrence. These results are presented in Figures 5 and 6 (page 9668) and Supplementary Figures 4 and 5 in the Cancer Research paper [34].

(2) We have extended our finding in LNCaP cells to three other prostate cancer cell lines (DU-145, PC-3 and VCaP). We observed that IR induced neurite extension and the expression of CgA and NSE to a lesser extent when compared with LNCaP cells. We also confirmed that IR also induced cytoplasmic sequestration of ATF2 and CREB phosphorylation in a subset of cells in DU-145 and PC-3. These results are now included in a recently submitted manuscript (see Figs. 1-4 in the attached manuscript).

(3) We have also initiated the collaboration with Dr. Tim Ratliff and Dr. Wally Morrison at Purdue to confirm that IR also induced NED in LNCaP xenograft tumors. More importantly, we found that IR elevated the plasma CgA level by 2-4 fold after 20 and 40 Gy of irradiation when compared with the plasma CgA level before radiation. This finding is very exciting given that CgA has been used to diagnose neuroendocrine tumors clinically. We hypothesize that monitoring plasma CgA will allow for evaluation of radiotherapy-induced NED and this may allow for the establishment of a clinical correlation between radiation-induced NED and clinical outcomes. Since we noticed that plasma CgA levels are affected by the tumor volume (no of tumor cells), we have recently measured plasma PSA levels and normalized CgA levels to PSA levels. In all irradiated tumor-bearing mice, we observed an average of 5-fold increase. This result along with the

immunohistochemical results are all included in the recently submitted manuscript (see Fig. 5 in the attached manuscript).

(4) Our exciting finding from *in vivo* studies prompted us to explore whether radiotherapy can induce NED in prostate cancer patients. For this purpose, we have collaborated with Dr. Song-Chu Ko at Indiana University School of Medicine to perform a pilot study. We enrolled 9 prostate cancer patients, and collected their blood samples before, in the middle of, and immediately after radiotherapy. We then measured serum CgA levels and PSA levels. Two patients showed elevation of serum CgA levels after radiotherapy. When normalized to serum PSA levels, 4 out of 9 patients (44%) showed 1.5-2.2 fold increase in serum CgA. This finding, along with our *in vitro* and *in vivo* studies, strongly suggests that radiotherapy can indeed induce NED in a subset of prostate cancer patients. Further detailed analysis of radiotherapy-induced NED in prostate cancer patients in a large scale study will likely provide new insight into the role of NED in the therapeutic responses and prognosis in prostate cancer patients. These results are also included as Fig. 6 in the newly submitted manuscript.

Key Research Accomplishments

- Demonstrated that 40 Gy of irradiation is sufficient to induce neurite extension in LNCaP cells
- Demonstrated that 40 Gy of irradiation can induce expression of two NE markers chromagranin A (CgA) and neuron specific enolase (NSE)
- Demonstrated that IR-induced NE-like cells show increased cytoplasmic localization of ATF2 and increased pCREB in the nucleus
- Demonstrated that 10 Gy of irradiation is enough to induce cytoplasmic sequestration of ATF2 and nuclear accumulation of pCREB
- Demonstrated that knockdown of ATF2 or overexpression of a constitutively cytoplasmic-localized ATF2 induces NED
- Demonstrated that overexpression of VP16-bCREB induces NED and its induction of NED can be attenuated by a constitutively nuclear-localized ATF2 (nATF2)
- Demonstrated that overexpression of nATF2 or CREB-S133A (dominant negative mutant of CREB) can inhibit IR-induced neurite outgrowth. However, only nATF2, but not CREB-S133A, inhibits IR-induced CgA and NSE expression.
- Demonstrated that IR-induced NED is reversible and dedifferentiated cells are cross-resistant to the treatments with radiation, androgen ablation and chemotherapeutic agent docetaxel.
- Demonstrated that CREB can activate the CgA reporter gene.
- Demonstrated that IR induced pCREB binding to CgA.
- Demonstrated that IR also induced neurite extension in DU-145, PC-3 and VCaP cells and the expression of CgA and NSE to certain extent.
- Demonstrated that IR induced CgA expression in LNCaP xenograft tumors.
- Demonstrated that IR increased plasma CgA levels in LNCaP xenograft tumor-bearing nude mice.
- Identified PKA as a potential protein kinase responsible for IR-induced CREB activation
- Identified CaMKII as a potential interacting protein of pCREB
- Demonstrated that A-CREB expression can sensitize LNCaP cells to IR.
- Showed that radiotherapy in prostate cancer patients can induce NED in 44% of patients.

Reportable Outcomes

1. Publication of research results in Cancer Research
   Deng, X., Liu, H., Huang, J., Cheng, L., Keller, E, Parsons, S.J. and Hu, C.D. Ionizing radiation induces prostate cancer cell neuroendocrine differentiation through interplay of CREB and ATF2: Implications for disease progression. *Cancer Res.* **68**:9663-9670 (2008)

2. Manuscript submitted to American Journal of Cancer Research
   Deng, X., Elzey B., Poulson, J., Morrison, W., Ko, S.C., Hahn, N., Ratliff, T., and Hu, CD. Ionizing radiation induces neuroendocrine differentiation in prostate cancer cells in vitro, in vivo, and in prostate cancer patients.

3. Meeting attendance
   The interplay of CREB and ATF2 in regulating ionizing radiation-induced neuroendocrine differentiation in prostate cancer cells
   Authors: Xuehong Deng[1], Han Liu[1], Jiaoti Huang[2], Liang Cheng[3], Evan T. Keller[4], Sarah J. Parsons[5], and Chang-Deng Hu[1]
   Meeting: Mechanisms and Models of Cancer
   Place and Date: Cold Spring Harbor, August 13-17, 2008

   Radiation induces neuroendocrine differentiation of prostate cancer cell lines in vitro and in vivo
   Authors: Chang-Deng Hu, Bennett Elzey, Jean Poulson, Wallace Morrison, Xuehong Deng, Sandra Torregrosa-Allen, Timothy Ratliff
   Meeting: 2010 AUA Meeting and SBUR meeting
   Place and Date: San Francisco, May 28-June 3, 2010

   Radiation induces neuroendocrine differentiation of prostate cancer cells *in vitro* and *in vivo:* Implications for prostate cancer radiotherapy
   Authors: Chang-Deng Hu, Xuehong Deng, Christopher Suarez, Bennett D. Elzey, Jean M. Poulson, Wallace B. Morrison, Sandra Torregrosa-Allen, Jiaoti Huang, Liang Cheng, Evan T. Keller, Sarah J. Parsons, Timothy L. Ratliff
   Meeting: 2011 IMPaCT
   Place and Date: Orlando, March 9-12, 2011

4. Invited Seminars (prostate cancer related only)
   (1) Ionizing radiation-induced neuroendocrine differentiation: implication in prostate cancer therapy
   Place: University of Virginia Cancer Center
   Date: December 18, 2008
   (2) Ionizing radiation-induced neuroendocrine differentiation: implication in prostate cancer therapy
   Place: Indiana University Medical School, Department of Bioehcmistry
   Date: February 2, 2009
   (3) Mechanisms and targeting of therapy-resistant prostate cancer

Place: Beijing University Cancer Hospital
Date: September 13, 2010

(4) Mechanisms and targeting of therapy-resistant prostate cancer
Place: Wannan Medical College
Date: September 25, 2010

(5) Mechanisms and targeting of therapy-resistant prostate cancer
Place: Tulane University
Time: February 8, 2010

5. Development of cell lines
We have isolated three radiation resistant clones LNCaP-IRR1, LNCaP-IRR2 and LNCaP-IRR3 from dedifferentiated cells. These clones will be useful for molecular mechanism study and for development of novel therapeutics. We have also recently isolated several sublines from DU-145 after 40 and 70 Gy of irradiation.

6. Funding applied and funded
Title: Targeting of prostate cancer transdifferentiation and proliferation via a novel DNA nanotube-based nucleic acid delivery
Agency: Lilly Seed Grant (School of Pharmacy and Pharmaceutical Sciences, Purdue)
Total Cost: $100,000
Period: Jan 2009 – Dec 2010

Title: Radiation-induced prostate cancer transdifferentiation *in vivo*
Agency: Purdue University Center for Cancer Research
PI: Chang-Deng Hu
Grant Period: 01/01/09-12/31/10
Total Cost: $23,400 (milestone-based funding for a total of $50,000)
Goals: The goal of this project is to use xenograft nude mice prostate cancer cell models to investigate whether CREB and ATF2 contribute to radiation-induced neuroendocrine differentiation *in vivo* and to determine whether radiation induces changes of pCREB and ATF2 subcellular localization.

Title: Chromogranin A: a biomarker to monitor radiotherapy-induced neuroendocrine differentiation and to predict prognosis
PI: Chang-Deng Hu
Grant Period: 07/01/2010-06/30/2011
Total Cost: $8,000
Goals: The goal of this pilot study is to measure serum CgA before, during and after radiotherapy from 20 prostate cancer patients. We will use the preliminary results to do power calculation for a large scale analysis. We have already obtained results from 9 patients and found that 4 out of 9 patients showed serum CgA elevation. This is sufficient for our purpose.

Conclusion

Under the support of this prostate cancer idea development award, we have demonstrated that ionizing radiation can induce neuroendocrine differentiation (NED) in the prostate cancer cells LNCaP, DU-145, PC-3 and VCaP. Furthermore, we have also shown that radiation also induced NED in LNCaP xenografted tumors in nude mice and increased plasma chromogranin A levels. We have shown that two CRE-binding transcription factors ATF2 and CREB plays an opposite role in neuroendocrine differentiation and that IR induces NED by impairing ATF2 nuclear import and promoting nuclear localization of phosphorylated CREB. Importantly, we have also shown that IR-induced NED is reversible and three radiation resistant clones derived from dedifferentiated cells are cross-resistant to radiation, androgen ablation and chemotherapy. Further evidence comes from the finding that IR increases the CgA reporter gene activity and induces pCREB binding to the CgA promoter. All of these together strongly support the ideat that CREB plays a critical role in IR-induced NED. We have provided evidence over the past year that targeting of CREB by a dominant negative CREB, A-CREB, can sensitize LNCaP cells to IR. These findings suggest that IR-induced NED may represent a novel pathway by which prostate cancer cells survive the treatment and contribute to recurrence. In addition, we have extended beyond the proposed experiments in the original submission and found that IR induced NED in three other prostate cancer cell lines and in LNCaP xenograft tumors in nude mice. Interestingly, we also observed that irradiation of LNCaP xenograft tumors in nude mice also increased the serum CgA level in mice. This finding suggests that serum CgA levels can be used as a biomarker to monitor radiotherapy-induced NED in prostate cancer patients. In fact, our pilot study with 9 prostate cancer patients has shown that 4 out of 9 patients showed serum CgA elevation after radiotherapy. Therefore, we are requesting for funding to develop a large scale study.

References

[1] Daneshmand S, Quek ML and Pinski J. Neuroendocrine differentiation in prostate cancer. Cancer Therapy 2005;3:383-396.

[2] Nelson EC, Cambio AJ, Yang JC, Ok JH, Lara PN, Jr. and Evans CP. Clinical implications of neuroendocrine differentiation in prostate cancer. Prostate Cancer Prostatic Dis 2007;10:6-14.

[3] Amorino GP and Parsons SJ. Neuroendocrine cells in prostate cancer. Crit Rev Eukaryot Gene Expr 2004;14:287-300.

[4] Yuan TC, Veeramani S and Lin MF. Neuroendocrine-like prostate cancer cells: neuroendocrine transdifferentiation of prostate adenocarcinoma cells. Endocr Relat Cancer 2007;14:531-47.

[5] Yuan TC, Veeramani S, Lin FF, Kondrikou D, Zelivianski S, Igawa T, Karan D, Batra SK and Lin MF. Androgen deprivation induces human prostate epithelial neuroendocrine differentiation of androgen-sensitive LNCaP cells. Endocr Relat Cancer 2006;13:151-67.

[6] Ismail AH, Landry F, Aprikian AG and Chevalier S. Androgen ablation promotes neuroendocrine cell differentiation in dog and human prostate. Prostate 2002;51:117-25.

[7] Wright ME, Tsai MJ and Aebersold R. Androgen receptor represses the neuroendocrine transdifferentiation process in prostate cancer cells. Mol Endocrinol 2003;17:1726-37.

[8] Jin RJ, Wang Y, Masumori N, Ishii K, Tsukamoto T, Shappell SB, Hayward SW, Kasper S and Matusik RJ. NE-10 neuroendocrine cancer promotes the LNCaP xenograft growth in castrated mice. Cancer Res 2004;64:5489-95.

[9] Jiborn T, Bjartell A and Abrahamsson PA. Neuroendocrine differentiation in prostatic carcinoma during hormonal treatment. Urology 1998;51:585-9.

[10] Zhang XQ, Kondrikov D, Yuan TC, Lin FF, Hansen J and Lin MF. Receptor protein tyrosine phosphatase alpha signaling is involved in androgen depletion-induced neuroendocrine differentiation of androgen-sensitive LNCaP human prostate cancer cells. Oncogene 2003;22:6704-16.

[11] Lee SO, Chun JY, Nadiminty N, Lou W and Gao AC. Interleukin-6 undergoes transition from growth inhibitor associated with neuroendocrine differentiation to stimulator accompanied by androgen receptor activation during LNCaP prostate cancer cell progression. Prostate 2007;67:764-73.

[12] Deeble PD, Murphy DJ, Parsons SJ and Cox ME. Interleukin-6- and cyclic AMP-mediated signaling potentiates neuroendocrine differentiation of LNCaP prostate tumor cells. Mol Cell Biol 2001;21:8471-82.

[13] Wang Q, Horiatis D and Pinski J. Interleukin-6 inhibits the growth of prostate cancer xenografts in mice by the process of neuroendocrine differentiation. Int J Cancer 2004;111:508-13.

[14] Xie S, Lin HK, Ni J, Yang L, Wang L, di Sant'Agnese PA and Chang C. Regulation of interleukin-6-mediated PI3K activation and neuroendocrine differentiation by androgen signaling in prostate cancer LNCaP cells. Prostate 2004;60:61-7.

[15] Spiotto MT and Chung TD. STAT3 mediates IL-6-induced neuroendocrine differentiation in prostate cancer cells. Prostate 2000;42:186-95.

[16] Qiu Y, Robinson D, Pretlow TG and Kung HJ. Etk/Bmx, a tyrosine kinase with a pleckstrin-homology domain, is an effector of phosphatidylinositol 3'-kinase and is involved in interleukin 6-induced neuroendocrine differentiation of prostate cancer cells. Proc Natl Acad Sci U S A 1998;95:3644-9.
[17] Cox ME, Deeble PD, Lakhani S and Parsons SJ. Acquisition of neuroendocrine characteristics by prostate tumor cells is reversible: implications for prostate cancer progression. Cancer Res 1999;59:3821-30.
[18] Farini D, Puglianiello A, Mammi C, Siracusa G and Moretti C. Dual effect of pituitary adenylate cyclase activating polypeptide on prostate tumor LNCaP cells: short- and long-term exposure affect proliferation and neuroendocrine differentiation. Endocrinology 2003;144:1631-43.
[19] Zelivianski S, Verni M, Moore C, Kondrikov D, Taylor R and Lin MF. Multipathways for transdifferentiation of human prostate cancer cells into neuroendocrine-like phenotype. Biochim Biophys Acta 2001;1539:28-43.
[20] Bang YJ, Pirnia F, Fang WG, Kang WK, Sartor O, Whitesell L, Ha MJ, Tsokos M, Sheahan MD, Nguyen P and et al. Terminal neuroendocrine differentiation of human prostate carcinoma cells in response to increased intracellular cyclic AMP. Proc Natl Acad Sci U S A 1994;91:5330-4.
[21] Vinson C, Myakishev M, Acharya A, Mir AA, Moll JR and Bonovich M. Classification of human B-ZIP proteins based on dimerization properties. Molecular & Cellular Biology 2002;22:6321-35.
[22] Ma Q, Li X, Vale-Cruz D, Brown ML, Beier F and Luvalle P. Activating transcription factor 2 controls Bcl-2 promoter activity in growth plate chondrocytes. J Cell Biochem 2007;101:477-87.
[23] Sangerman J, Lee MS, Yao X, Oteng E, Hsiao CH, Li W, Zein S, Ofori-Acquah SF and Pace BS. Mechanism for fetal hemoglobin induction by histone deacetylase inhibitors involves gamma-globin activation by CREB1 and ATF-2. Blood 2006;108:3590-9.
[24] Gueorguiev VD, Cheng SY and Sabban EL. Prolonged activation of cAMP-response element-binding protein and ATF-2 needed for nicotine-triggered elevation of tyrosine hydroxylase gene transcription in PC12 cells. J Biol Chem 2006;281:10188-95.
[25] Ionescu AM, Drissi H, Schwarz EM, Kato M, Puzas JE, McCance DJ, Rosier RN, Zuscik MJ and O'Keefe RJ. CREB Cooperates with BMP-stimulated Smad signaling to enhance transcription of the Smad6 promoter. J Cell Physiol 2004;198:428-40.
[26] Ionescu AM, Schwarz EM, Zuscik MJ, Drissi H, Puzas JE, Rosier RN and O'Keefe RJ. ATF-2 cooperates with Smad3 to mediate TGF-beta effects on chondrocyte maturation. Exp Cell Res 2003;288:198-207.
[27] Niwano K, Arai M, Koitabashi N, Hara S, Watanabe A, Sekiguchi K, Tanaka T, Iso T and Kurabayashi M. Competitive binding of CREB and ATF2 to cAMP/ATF responsive element regulates eNOS gene expression in endothelial cells. Arterioscler Thromb Vasc Biol 2006;26:1036-42.
[28] Flint KJ and Jones NC. Differential regulation of three members of the ATF/CREB family of DNA-binding proteins. Oncogene 1991;6:2019-26.
[29] Hay CW, Ferguson LA and Docherty K. ATF-2 stimulates the human insulin promoter through the conserved CRE2 sequence. Biochim Biophys Acta 2007;1769:79-91.

[30] Garcia GE, Nicole A, Bhaskaran S, Gupta A, Kyprianou N and Kumar AP. Akt-and CREB-mediated prostate cancer cell proliferation inhibition by Nexrutine, a Phellodendron amurense extract. Neoplasia 2006;8:523-33.
[31] Unni E, Sun S, Nan B, McPhaul MJ, Cheskis B, Mancini MA and Marcelli M. Changes in androgen receptor nongenotropic signaling correlate with transition of LNCaP cells to androgen independence. Cancer Res 2004;64:7156-68.
[32] Canaff L, Bevan S, Wheeler DG, Mouland AJ, Rehfuss RP, White JH and Hendy GN. Analysis of molecular mechanisms controlling neuroendocrine cell specific transcription of the chromogranin A gene. Endocrinology 1998;139:1184-96.
[33] Kim J, Jia L, Stallcup MR and Coetzee GA. The role of protein kinase A pathway and cAMP responsive element-binding protein in androgen receptor-mediated transcription at the prostate-specific antigen locus. J Mol Endocrinol 2005;34:107-18.
[34] Deng X, Liu H, Huang J, Cheng L, Keller ET, Parsons SJ and Hu CD. Ionizing radiation induces prostate cancer neuroendocrine differentiation through interplay of CREB and ATF2: Implications for disease progression. Cancer Res. 2008;68:9663-9670.
[35] Johannessen M and Moens U. Multisite phosphorylation of the cAMP response element-binding protein (CREB) by a diversity of protein kinases. Front Biosci 2007;12:1814-32.
[36] Ahn S, Olive M, Aggarwal S, Krylov D, Ginty DD and Vinson C. A dominant-negative inhibitor of CREB reveals that it is a general mediator of stimulus-dependent transcription of c-fos. Mol Cell Biol 1998;18:967-77.
[37] Impey S, McCorkle SR, Cha-Molstad H, Dwyer JM, Yochum GS, Boss JM, McWeeney S, Dunn JJ, Mandel G and Goodman RH. Defining the CREB regulon: a genome-wide analysis of transcription factor regulatory regions. Cell 2004;119:1041-54.

Appendices

1. Cancer Research paper (2008).
2. Manuscript reporting findings in other prostate cancer cells, in xenograft nude mouse models and in human patients.
3. Figures 1-8.

Ionizing Radiation Induces Prostate Cancer Neuroendocrine Differentiation through Interplay of CREB and ATF2: Implications for Disease Progression

Xuehong Deng,[1] Han Liu,[1] Jiaoti Huang,[2] Liang Cheng,[3] Evan T. Keller,[4] Sarah J. Parsons,[5] and Chang-Deng Hu[1]

[1]Department of Medicinal Chemistry and Molecular Pharmacology and the Purdue Cancer Center, Purdue University, West Lafayette, Indiana; [2]Department of Pathology, University of Rochester Medical Center, Rochester, New York; [3]Department of Pathology and Laboratory Medicine, Indiana University School of Medicine, Indianapolis, Indiana; [4]Department of Urology, University of Michigan, Ann Arbor, Michigan; and [5]Department of Microbiology, University of Virginia Health System, Charlottesville, Virginia

Abstract

Radiation therapy is a first-line treatment for prostate cancer patients with localized tumors. Although some patients respond well to the treatment, ~10% of low-risk and up to 60% of high-risk prostate cancer patients experience recurrent tumors. However, the molecular mechanisms underlying tumor recurrence remain largely unknown. Here we show that fractionated ionizing radiation (IR) induces differentiation of LNCaP prostate cancer cells into neuroendocrine (NE)-like cells, which are known to be implicated in prostate cancer progression, androgen-independent growth, and poor prognosis. Further analyses revealed that two cyclic AMP–responsive element binding transcription factors, cyclic AMP–response element binding protein (CREB) and activating transcription factor 2 (ATF2), function as a transcriptional activator and a repressor, respectively, of NE-like differentiation and that IR induces NE-like differentiation by increasing the nuclear content of phospho-CREB and cytoplasmic accumulation of ATF2. Consistent with this notion, stable expression of a non-phosphorylatable CREB or a constitutively nuclear-localized ATF2 in LNCaP cells inhibits IR-induced NE-like differentiation. IR-induced NE-like morphologies are reversible, and three IR-resistant clones isolated from dedifferentiated cells have acquired the ability to proliferate and lost the NE-like cell properties. In addition, these three IR-resistant clones exhibit differential responses to IR- and androgen depletion–induced NE-like differentiation. However, they are all resistant to cell death induced by IR and the chemotherapeutic agent docetaxel and to androgen depletion–induced growth inhibition. These results suggest that radiation therapy–induced NE-like differentiation may represent a novel pathway by which prostate cancer cells survive the treatment and contribute to tumor recurrence. [Cancer Res 2008;68(23):9663–70]

Introduction

Radiation therapy is a first-line treatment for prostate cancer. Although some patients with localized tumors respond well to the treatment (1), ~10% of low-risk and up to 60% of high-risk prostate cancer patients experience recurrent tumors (2). However, the molecular mechanisms underlying tumor recurrence remain largely unknown.

Neuroendocrine (NE) cells are one of three types of epithelial cells in the human prostate and are present in 30% to 100% cases of prostatic adenocarcinoma (3, 4). Although the physiologic role of NE cells remains unclear, increased numbers of NE-like cells seem to be associated with prostate cancer progression, androgen-independent growth, and poor prognosis (5, 6). Interestingly, androgen ablation, cytokines such as interleukin 6 (IL-6), and agents that elevate the intracellular levels of cyclic AMP (cAMP) can induce NE-like differentiation (NED) in LNCaP prostate cancer cells by activating several distinct signaling pathways (5, 6). Like NE cells, the differentiated NE-like cells also produce a number of neuropeptides that facilitate the growth of surrounding tumor cells in a paracrine manner (5–7). They are generally androgen receptor negative (8, 9), highly resistant to apoptosis (10, 11), and their differentiation state is reversible (12). Thus, NE-like cells may survive in a dormant state and contribute to prostate cancer recurrence on dedifferentiation (12).

cAMP response element binding protein (CREB) belongs to the basic region leucine zipper (bZIP) family of transcription factors (13–15). It functions as a homodimer or heterodimer to bind a specific DNA sequence, the cAMP responsive element (16), to regulate transcription of target genes responsible for many cellular processes including cell proliferation and differentiation (15). CREB is implicated in prostate cancer growth (17), acquisition of androgen-independent growth (18), and transcription of chromogranin A (CgA; ref. 19) and prostate-specific antigen (20). Although it is known that CREB is activated by protein kinase A through the phosphorylation at Ser^{133} of CREB1B in response to cAMP (14, 21), whether CREB itself can induce NED remains to be determined.

Activating transcription factor 2 (ATF2) also belongs to the bZIP family of transcription factors (22, 23) and is a member of the activator protein 1 (AP-1; ref. 24). AP-1 activity is required for many cellular processes, and deregulated AP-1 activity is implicated in many cancers including prostate cancer (25). Interestingly, ATF2 and CREB share the same cAMP responsive element sequence and regulate the transcription of cAMP responsive element–containing genes. Whereas some cAMP responsive element–containing target

Note: Supplementary data for this article are available at Cancer Research Online (http://cancerres.aacrjournals.org/).

Requests for reprints: Chang-Deng Hu, Department of Medicinal Chemistry and Molecular Pharmacology, Purdue University, West Lafayette, IN 47907. Phone: 765-496-1971; Fax: 765-494-1414; E-mail: cdhu@pharmacy.purdue.edu.

doi:10.1158/0008-5472.CAN-08-2229

genes are activated by CREB and ATF2 equally or cooperatively (26), differential regulation of other target genes by CREB and ATF2 has also been observed (27–31). Unlike CREB, the role of ATF2 in prostate cancer is little known. A recent study reported that increased cytoplasmic localization of phospho-ATF2 in prostate cancer specimens correlates with the clinical progression of prostate cancer (32), suggesting that alteration of ATF2 subcellular localization may contribute to clinical progression of prostate cancer.

We recently showed that ATF2 is a nucleocytoplasmic shuttling protein and its subcellular localization is regulated by AP-1 dimerization (33). Here we present evidence that ATF2 constantly shuttles between the cytoplasm and nucleus in proliferating LNCaP cells and that fractionated ionizing radiation (IR) induces NED by impairing the nuclear import of ATF2 and increasing the nuclear phospho-CREB at Ser^{133} (pCREB).

Materials and Methods

Plasmid construction. To construct a constitutively activated form of CREB, cDNA encoding residues 413 to 490 of VP16 was amplified by PCR from VP16 (Clontech) and subcloned into pHA-CMV. To make VP16-bCREB fusion proteins, cDNA encoding the bZIP domain of CREB1B (residues 285–314) was amplified by PCR from a human cDNA library and subcloned into pHA-VP16. A flexible glycine spacer ($GGGGSx_4$) was inserted between VP16 and bCREB. For the construction of nuclear-localized ATF2 (nATF2), the sequence encoding a nuclear localization signal (PKKKRKV) from the large T antigen of SV40 (34) was subcloned upstream of ATF2 coding sequences in pFlag-ATF2. pFlag-cATF2 is a deletion mutant of ATF2 in which two nuclear localization signals are deleted (33). Both cytoplasmic-localized ATF2 (cATF2) and nATF2 were expressed as a fusion protein with the fluorescent protein, Venus, in transient transfection experiments. To knock down ATF2, sense and antisense oligos (19-mer) were synthesized and subcloned into pSUPER (OligoEngine). Four short interference RNA (siRNA) constructs were made, and their effect on ATF2 expression in LNCaP cells was verified by transient transfection, followed by immunoblotting of ATF2. One ATF2 siRNA construct targeting the 5′ untranslated region (148–167 of ATF2 mRNA) proved to be the most potent and was used in this work. All plasmids were verified by DNA sequencing.

IR-induced NE-like differentiation. Cells were cultured in 10-cm dishes in RPMI 1640 supplemented with 10% fetal bovine serum (FBS) and antibiotics and were continuously irradiated (2 Gy/d, 5 d/wk) in a GC-220 Co-60 for the indicated times. NE-like cells were visualized by morphologic changes, and the induction of the NE markers, CgA and neuron-specific enolase (NSE), was determined by immunoblotting with anti-CgA and anti-NSE antibodies (Abcam). To determine the effect of CREB-S133A and nATF2 on IR-induced NED, we used a tetracycline-on system (Invitrogen) to establish stable cell lines that inducibly expressed HA-CREB-S133A or Flag-nATF2. The established cell lines were maintained in the presence of selectable markers (zeocin and blasticidin), and 5 μg/mL tetracycline was applied while cells were irradiated as described above. Media were changed twice a week, and antibiotics and tetracycline were added accordingly. Cells that extended neurites longer than two cell bodies were scored as differentiated, and the induction of CgA and NSE was analyzed by immunoblotting and quantified using ImageJ software. Values were normalized to β-actin.

Analysis of ATF2 and CREB subcellular localization. LNCaP cells were fixed in ice-cold 3.7% formaldehyde for 20 min, followed by permeabilization in ice-cold 0.2% Triton X-100 for 5 min. Cells were incubated with anti-ATF2 (c-19; Santa Cruz Biotechnology) overnight, followed by three washes and incubation with the secondary antibody conjugated with Texas red (Jackson ImmunoResearch Laboratories) for 1 h. To stain DNA, 4′,6-diamidino-2-phenylindole (DAPI) was added to the secondary antibody staining reaction at the final concentration of 0.5 μg/mL. Subcelluar localization of ATF2 was examined by microscopic analysis, and fluorescent images were captured using a charge-coupled device camera mounted on a Nikon TE2000 inverted fluorescence microscope with the DAPI and Texas red filters.

For biochemical subcellular fractionation analysis, cytosolic and nuclear fractions were prepared as described before (33). Cytosolic and nuclear fractions were verified by anti–β-tubulin (Sigma) or anti–histone 3 (Abcam), respectively, in immunoblotting assays. The amounts of ATF2, pCREB, and CREB were determined with anti-ATF2, anti-pCREB, and anti-CREB (Cell Signaling) antibodies. The amounts of ATF2 and pCREB in the cytoplasm or nucleus, respectively, relative to total protein were quantified using ImageJ software.

Transient transfection. To evaluate the effect of ATF2 knockdown, mutant ATF2, or mutant CREB on NED, 60% to 80% confluent LNCaP cells cultured in 10-cm dishes were transfected with the indicated plasmids using FuGENE HD (Roche). Transfected cells were examined for morphologic changes and harvested for determination of expression of NE markers CgA and NSE by immunoblotting 6 d after transfection. The induction of CgA and NSE was quantified using ImageJ software and normalized to β-actin.

IR- and androgen depletion–induced NE-like differentiation in IR-resistant clones. To study IR-induced NED in IR-resistant clones, cells were similarly treated as described above for wild-type LNCaP cells. NE-like cells were visualized by morphologic changes, and the induction of NE markers CgA and NSE and the expression of androgen receptor were determined by immunoblotting with anti-CgA, anti-NSE, and anti–androgen receptor (Santa Cruz Biotechnology) antibodies. To determine the response of IR-resistant clones to androgen depletion treatment, cells were cultured in phenol-free RPMI 1640 supplemented with 10% charcoal-dextran–treated FBS (CD-FBS) for 3 wk and similarly assayed for morphologic changes and the induction of NE markers CgA and NSE. Note that although androgen depletion treatment for 1 wk was sufficient to induce neurite outgrowth, the induction of CgA and NSE expression was barely detectable by immunoblotting even for wild-type LNCaP cells.

Cell viability and growth inhibition assay. Wild-type or IR-resistant clones were cultured in 48-well plates and irradiated with fractionated IR (2 Gy/d) or treated with docetaxel (5 nmol/L) or cultured in phenol-free RPMI 1640 supplemented with 10% CD-FBS for the indicated times. Cell viability for IR- and docetaxel-treated cells was determined by a 3-(4,5-dimethylthiazol-2-yl)-2,5-diphenyltetrazolium bromide assay as described previously (33). Because irradiated cells only showed cell death starting from the 2nd week of irradiation, the cell viability of wild-type LNCaP or IR-resistant clones was determined by comparing to cells that had received 10-Gy irradiation. Because wild-type and IR-resistant clones showed different growth rates and because CD-FBS treatment only inhibited cell growth without inducing cell death, cells cultured in normal FBS were used as controls to first calculate the percentage of growth inhibition (percentage of viable cells in CD-FBS over those in normal FBS), which was subsequently used to calculate the percentage of growth inhibition at different times when compared with cells immediately after treatment (day 0). A Student's *t* test was applied for statistical analysis.

Results

IR induces NE-like differentiation in LNCaP cells. In an attempt to isolate radiation-resistant clones by following a clinical protocol (70 Gy; ref. 1), we surprisingly found that on 40-Gy irradiation (2 Gy/d, 5 d/wk), the majority of cells (~80%) died whereas cells that survived the treatment displayed the growth of extended neurites (Fig. 1*A*), a NE-like phenotype. Expression of two NE cell markers, CgA and NSE, was significantly induced (Fig. 1*B* and *C*). Similar treatments failed to induce NED in DU145 and PC-3 prostate cancer cells. Consistent with previous reports that NE cells are apoptosis resistant (10, 11), IR-induced NE-like cells were resistant to IR and survived another 3-wk irradiation until the completion of the entire radiation protocol (70 Gy). Addition of the chemotherapeutic agent docetaxel into the IR-induced NE-like cells did not cause any change in cell viability either.

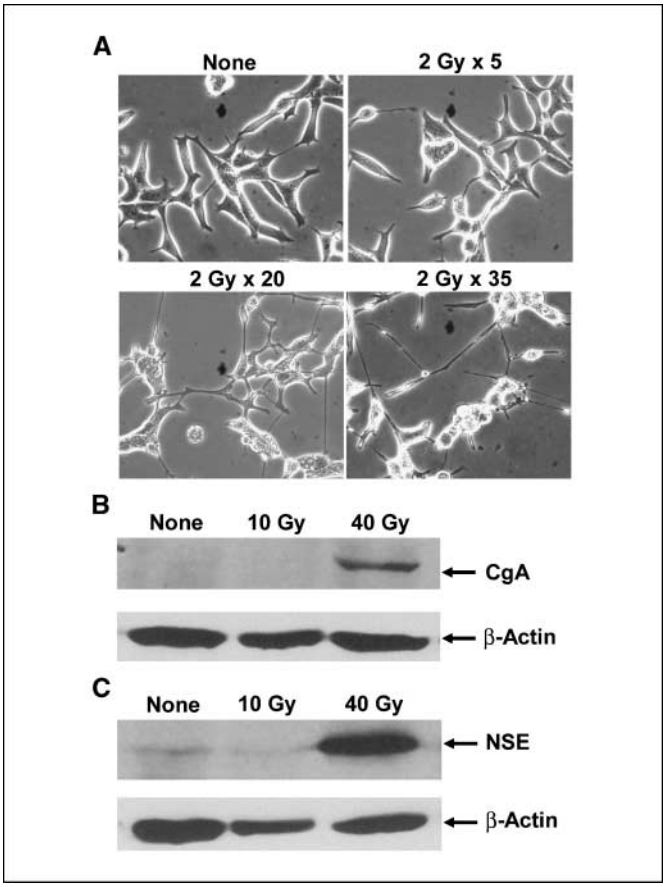

Figure 1. IR induces NE-like differentiation in LNCaP prostate cancer cells. *A,* representative images of cells that received the indicated times of exposures (2 Gy/d, 5 d/wk). Note that cells irradiated 20 times display significant neurite outgrowth and branching. *B* and *C,* immunoblotting of CgA and NSE. Cells that received the indicated dose of radiation were harvested and 20 μg of total protein was used for immunoblotting of CgA and NSE.

IR induces cytoplasmic accumulation of ATF2 and an increase in nuclear pCREB. To determine the subcellular localization of ATF2 in IR-induced NE-like cells, we performed immunostaining and found that ATF2 localization in the cytoplasm was increased compared with nontreated cells (Supplementary Fig. S1*A*). No significant changes in expression and nuclear localization of c-Jun, JunB, and JunD were observed (data not shown), suggesting that the increased cytoplasmic localization of ATF2 is not due to a decrease in Jun proteins to anchor ATF2 in the nucleus (33). In contrast, ATF2 was predominantly localized in the nucleus with some cytoplasmic localization in proliferating LNCaP cells, and treatment with the nuclear export inhibitor leptomycin B (33, 35) increased nuclear localization of ATF2 (Fig. 2*A*). The nuclear sequestration of ATF2 in proliferating LNCaP cells by leptomycin B was also confirmed by subcellular fractionation analysis (data not shown). These results show that ATF2 constantly shuttles between the cytoplasm and nucleus in proliferating LNCaP cells. Consistent with our previous observation that phosphorylation at residues T69 and T71 does not regulate ATF2 subcellular localization (33), the subcellular localization of phospho-ATF2 was similar to that of ATF2 in proliferating and the NE-like cells (data not shown).

To determine whether ATF2 cytoplasmic localization is a consequence or a potential cause of NED, we examined ATF2 subcellular localization at different time points before cells underwent morphologic changes. Irradiation of cells up to five times increased cytoplasmic ATF2 without inducing striking morphologic alterations (Fig. 2*A*). However, treatment of the irradiated cells with leptomycin B failed to induce nuclear accumulation of ATF2 in irradiated cells (Fig. 2*A*), indicating that IR impairs the nuclear import of ATF2. No significant change in ATF2 subcellular localization was observed when irradiated less than five times. Subcellular fractionation analysis showed that IR treatment increased cytoplasmic ATF2 from 24% to 45% of total ATF2 (Fig. 2*B*).

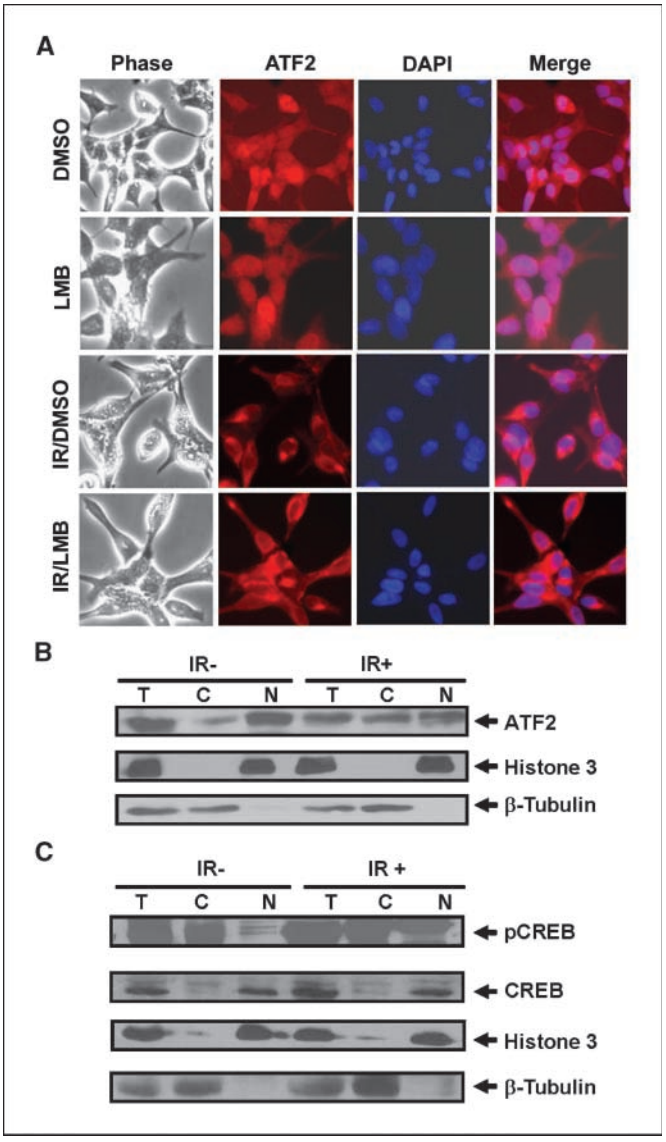

Figure 2. IR induces cytoplasmic accumulation of ATF2 and an increase in nuclear pCREB in LNCaP cells. *A,* LNCaP prostate cancer cells cultured in 12-well plates were treated with DMSO or leptomycin B (*LMB*; 40 ng/mL) overnight or irradiated (2 Gy/d) for 5 d, followed by treatment with DMSO or leptomycin B overnight. Subcellular localization of ATF2 was determined by immunostaining with anti-ATF2 antibody, and DNA in the nucleus was stained with DAPI. *B* and *C,* nonirradiated (*IR−*) or irradiated (2 Gy × 5; *IR+*) LNCaP cells were harvested, and cytosolic, nuclear, and total cellular extracts were prepared. Approximately 20 μg of total cellular extracts (*T*) and an equal portion of cytosolic (*C*) and nuclear (*N*) extracts were used for immunoblotting of ATF2, pCREB, and CREB.

Because CREB regulates transcription of CgA (19), we examined expression and subcellular localization of CREB and pCREB in proliferating and IR-irradiated cells, as we did for ATF2. Because all available pCREB antibodies we tested cross-reacted with phospho-ATF1 and another ~80-kDa cytoplasmic protein (data not shown), we performed subcellular fractionation analysis and determined that IR treatment increased nuclear pCREB from 25% to 49% of the total pCREB (Fig. 2*C*). Unlike pCREB, the nuclear content of CREB was not altered by IR treatment (Fig. 2*C*). Interestingly, pCREB was also detected in the cytoplasm in proliferating LNCaP cells, and IR treatment did not seem to alter the phosphorylation extent of cytoplasmic CREB. IR-induced NE-like cells maintained a high level of pCREB in the nucleus (Supplementary Fig. S1*B*). Taken together, these results show that IR-induced cytoplasmic accumulation of ATF2 and increase in nuclear pCREB occur before cells undergo differentiation.

CREB and ATF2 play opposing roles in NE-like differentiation. The IR-induced cytoplasmic accumulation of ATF2 and increase in nuclear pCREB prompted us to test the hypothesis that nuclear CREB and ATF2 may play opposing roles in NED. Indeed, 50% knockdown of ATF2 resulted in a NE-like morphologic change (Supplementary Fig. S2*A*) and a 1.6-fold induction of NSE (Fig. 3*A*). No induction of CgA was observed (data not shown). In contrast, transient expression of VP16-bCREB, a constitutively activated and nuclear-localized mutant of CREB (36, 37), induced a NE-like morphologic change (Supplementary Fig. S2*B*) and increased CgA and NSE expression by 2- to 3-fold (Fig. 3*B*). However, overexpression of a constitutively nuclear-localized ATF2 (nATF2), which has a nuclear localization signal from the large T antigen of SV40 fused to the NH_2 terminus of ATF2 as others did (34), inhibited VP16-bCREB–mediated morphologic changes and the induction of NSE. To determine whether increased cytoplasmic accumulation of endogenous ATF2 can induce NED, we overexpressed a constitutively cytoplasmic-localized ATF2 (cATF2), which lacks the two nuclear localization signals (33), in LNCaP cells. Because ATF2 homodimerization impairs ATF2 nuclear import (33), overexpression of cATF2 increased cytoplasmic localization of ATF2 to ~50% of total ATF2 (data not shown). Indeed, cATF2, but not nATF2, induced neurite outgrowth (Supplementary Fig. S2*C*) and a 5.4-fold increase in NSE expression (Fig. 3*C*). No induction of CgA by cATF2 or nATF2 was observed. Transiently expressed cATF2-Venus and nATF2-Venus were predominantly localized to the cytoplasm and nucleus, respectively (Supplementary Fig. S2*D*). Immunoblotting analysis confirmed the exogenous expression of VP16-bCREB, cATF2-Venus, and nATF2-Venus in these experiments (data not shown). Knockdown of ATF2 or expression of cATF2 had no effect on the localization and amount of pCREB, and overexpression of VP16-bCREB did not alter subcellular localization of ATF2 (data not shown). Taken together, these results support the hypothesis that CREB and ATF2 play opposing roles in NED.

Stable expression of a nonphosphorylatable CREB or nATF2 inhibits IR-induced NE-like differentiation. To further determine the role of CREB and ATF2 in IR-induced NED, we established tetracycline-inducible stable cell lines that express nATF2 or a nonphosphorylatable CREB (CREB-S133A), which has been used as a dominant negative mutant form of CREB (13, 15). In the absence of tetracycline, these stable cell lines exhibited normal morphology like vector-only cells (Fig. 4*A*). However, addition of tetracycline significantly induced expression of CREB-S133A or nATF2 (Fig. 4*B*) and reduced the percentage of cells displaying extended neurites in response to irradiation (Fig. 4*C*).

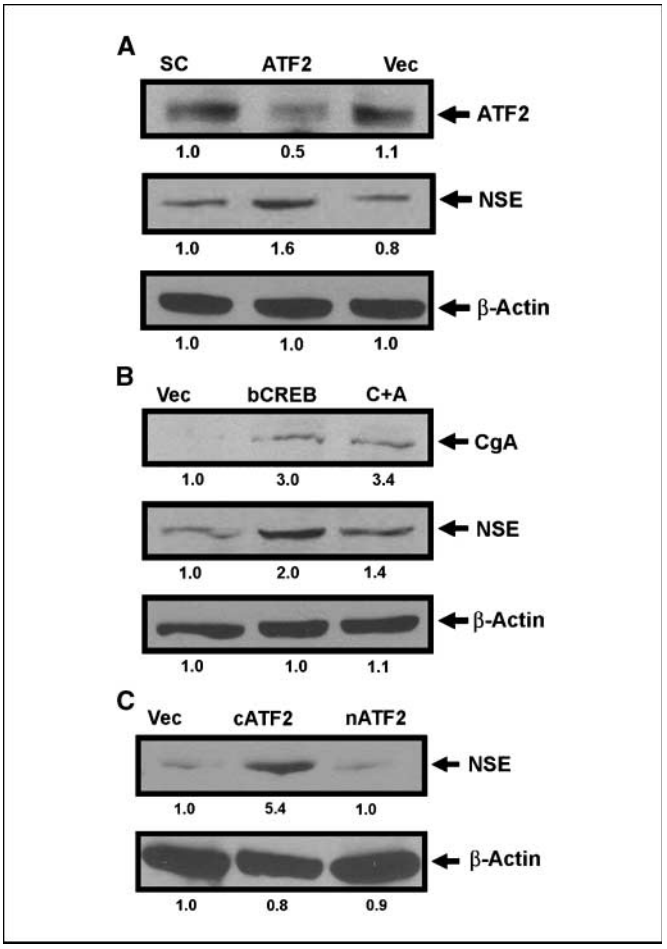

Figure 3. ATF2 and CREB play opposing roles in NE-like differentiation. *A,* immunoblotting analysis of ATF2 and NSE expression from LNCaP cells transfected with siRNA constructs for scrambled sequences (*SC*), ATF2 siRNA (*ATF2*), or pSUPER vector only (*Vec*). *B,* immunoblotting analysis of CgA and NSE from LNCaP cells transfected with the vector control (*Vec*), the plasmid encoding VP16-bCREB (*bCREB*), or cotransfected with plasmids encoding VP16-bCREB and nATF2 (*C+A*). *C,* immunoblotting analysis of NSE from LNCaP cells transfected with the vector control (*Vec*) or the plasmid encoding cATF2 or nATF2. The number below each lane is the quantified fold change when compared with the first lane.

Interestingly, induction of CgA and NSE by IR was inhibited by nATF2, but not by CREB-S133A (Fig. 4*D*). These results further support the conclusion that nuclear ATF2 and pCREB play different roles in IR-induced neurite outgrowth.

To determine the relationship between the expression of nATF2 and IR-induced phosphorylation of CREB and the relationship between the expression of CREB-S133A and the subcellular localization of ATF2, we irradiated cells for 5 days while constantly inducing expression of nATF2 or CREB-S133A. Expression of CREB-S133A did not affect IR-induced cytoplasmic localization of ATF2 (data not shown), whereas expression of nATF2 significantly inhibited IR-induced phosphorylation of CREB (Supplementary Fig. S3). However, expression of nATF2 only did not affect phosphorylation of CREB in the absence of IR (data not shown). These results suggest that IR-induced cytoplasmic sequestration of ATF2 may be a prerequisite for IR-induced phosphorylation of CREB and the subsequent NE-like differentiation.

IR-induced NE-like differentiation is reversible, and dedifferentiated cells lose NE-like properties. Because cAMP-induced

NE-like cells are reversible (12), we sought to determine whether IR-induced NE-like cells are also reversible. We irradiated cells for 4 weeks (40 Gy) to allow all surviving cells to differentiate into NE-like cells and then waited for the growth of any cells that were reversible. Although differentiated NE-like cells were maintained without obvious cell death or growth for the first 2 months, we isolated three independent clones 3 months after the completion of the irradiation. We named these clones LNCaP-IRR1 (IRR refers to IR resistant), LNCaP-IRR2, and LNCaP-IRR3. These IR-resistant cells showed similar morphology to wild-type LNCaP cells (Supplementary Fig. S4). All three clones lost CgA and NSE expression but retained levels of androgen receptor comparable to wild-type LNCaP cells (Fig. 5*A*), suggesting that these clones have lost their NE-like cell properties.

To determine whether these IR-resistant clones can still be induced to redifferentiation, we irradiated them at 40 Gy and examined for morphologic changes and the induction of CgA and NSE. Whereas all three clones exhibited extended neurite outgrowth (Supplementary Fig. S5*A*), the induction of CgA and NSE was completely abrogated (Fig. 5*A*). Interestingly, androgen receptor expression in LNCaP-IRR2 clone was significantly inhibited like in parental cells whereas androgen receptor expression in LNCaP-IRR1 and LNCaP-IRR3 cells was only slightly attenuated. These distinct responses to IR treatment suggest that these three IR-resistant clones are likely heterogeneous. To determine how these clones respond to androgen depletion treatment, we treated cells in phenol-free medium supplemented with 10% CD-FBS for 3 weeks. Whereas LNCaP-IRR1 and LNCaP-IRR3 cells exhibited extended neurite outgrowth, LNCaP-IRR2 cells showed only short neurites (Supplementary Fig. S5*B*). Interestingly, an induction of CgA expression by CD-FBS similar to parental cells was observed in LNCaP-IRR2; no induction was observed in LNCaP-IRR1; and a significantly attenuated induction was seen in LNCaP-IRR3 cells (Fig. 5*B*). On the contrary, the induction of NSE in LNCaP-IRR2 was abolished, whereas LNCaP-IRR1 and IRR3 responded to the treatment to some extent. Like the parental cells, however, the expression of androgen receptor in all three clones was significantly down-regulated by the CD-FBS treatment. Taken together, these results suggest that the three IR-resistant clones are heterogeneous and likely have distinct molecular defects in their responses to IR and androgen depletion treatments.

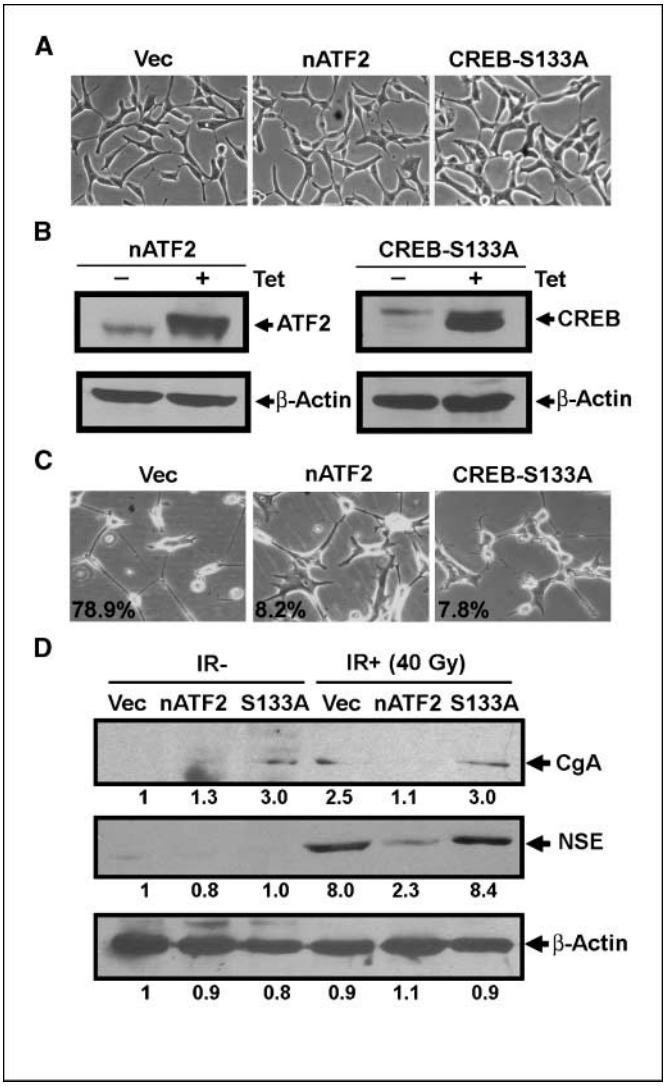

Figure 4. Inhibition of IR-induced NE-like differentiation by dominant negative CREB and nATF2. *A,* representative images of stable cell lines that have pcDNA4/TO (*Vec*), pcDNA4-TO-Flag-nATF2 (*nATF2*), or pcDNA4/TO-HA-CREB-S133A (*CREB-S133A*) integrated. *B,* immunoblotting analysis of induced nATF2 and CREB-S133A by tetracycline. Total cell lysates were prepared 3 d after the induction, and Flag-nATF2 and HA-CREB-S133A were detected with anti-ATF2 and anti-HA antibodies, respectively. *C,* representative images acquired from stable cell lines that received 40-Gy irradiation in the presence of tetracycline. The number indicates the percentage of cells showing extended neurites. *D,* immunoblotting analysis of CgA and NSE from experiments in *C*. The number below each lane is the quantified fold change when compared with the first lane.

IR-resistant and dedifferentiated cells acquire cross-resistance to therapy. To explore the potential implication of dedifferentiated cells in prostate cancer progression, we examined their response to radiation, the chemotherapeutic agent docetaxel (38), and androgen depletion treatments. Like the parental LNCaP cells, all three clones stopped growth during the 1st week of irradiation (10 Gy) and no cell death was observed (Fig. 6*A*). During the 2nd week of irradiation, however, all three clones showed significantly reduced cell death when compared with the parental cells. Interestingly, all three IR-resistant cells began to resume growth during the 3rd week of irradiation whereas the parental cells did not show obvious growth or death as all surviving cells differentiated into NE-like cells. Similar to their response to IR treatment, all three IR-resistant clones were resistant to cell death induced by the chemotherapeutic agent docetaxel (Fig. 6*B*), as well as to growth inhibition on androgen depletion (Fig. 6*C*). These results suggest that IR-induced NE-like cells have the potential to dedifferentiate back into a proliferating state with the acquisition of cross-resistance to radiotherapy, chemotherapy, and hormonal therapy.

Discussion

NE-like cells are implicated in prostate cancer progression, androgen-independent growth, and poor prognosis (3–6, 39, 40). Because androgen ablation treatment can induce NED *in vitro* and *in vivo* (3–6), it has been proposed that the presence of NE-like cells may contribute to androgen-independent growth, a critical factor leading to the failure of current prostate cancer therapy. We present here the first evidence that in addition to androgen ablation, IR also induces NED in the prostate cancer cell line LNCaP.

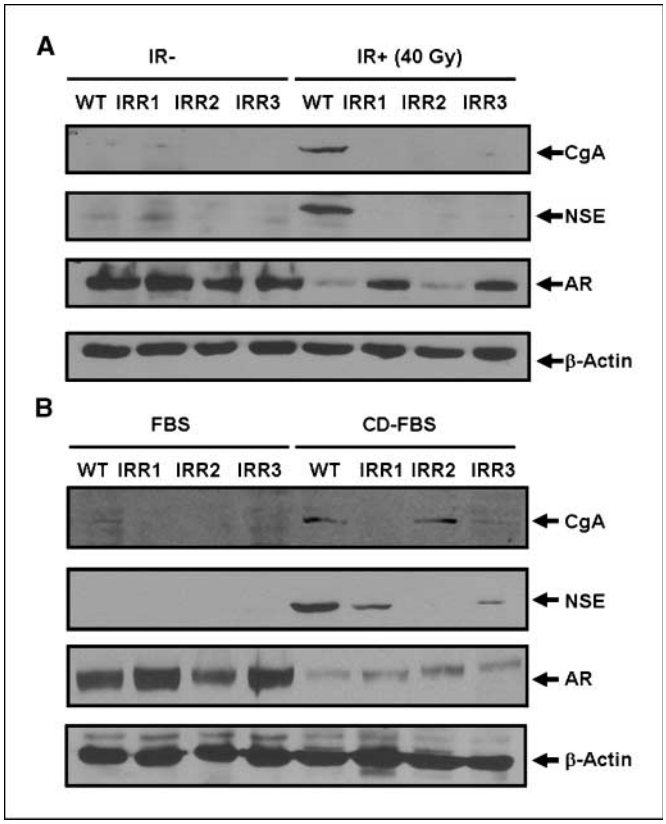

Figure 5. Response of IR-resistant clones to IR- and androgen depletion–induced NE-like redifferentiation. *A,* wild-type LNCaP (*WT*) and the indicated IR-resistant clones were subjected to fractionated IR (40 Gy), and the induction of CgA and NSE as well as the expression of androgen receptor (*AR*) was compared with that of nonirradiated cells. *B,* wild-type LNCaP and IR-resistant clones were cultured in medium supplemented with 10% FBS or CD-FBS for 3 wk, and the induction of CgA and NSE as well as the expression of androgen receptor was determined by immunoblotting.

Significantly, IR-induced NED is reversible, and dedifferentiated cells have lost the NE-like properties. However, all isolated three IR-resistant clones derived from dedifferentiated cells are cross-resistant to radiation, docetaxel, and androgen depletion treatments. These findings, along with other reports (41–46), strongly suggest that radiation- or hormonal therapy–induced NED may represent a common pathway by which cancer cells survive treatment and contribute to prostate cancer recurrence.

Although it has been reported that signal transducer and activator of transcription-3 (47) and β-catenin (48) can mediate IL-6– and androgen depletion–induced NED in prostate cancer cells, respectively, it remains largely unexplored how the switch from proliferation to differentiation is turned on at the transcriptional level. Several pieces of evidence presented in this work show that CREB functions as a transcriptional activator and ATF2 acts as a transcriptional repressor of NED. First, IR induced cytoplasmic accumulation of ATF2 and increased nuclear pCREB. Second, knockdown of ATF2 or overexpression of VP16-bCREB induced NED. Third, overexpression of nATF2 inhibited NED induced by VP16-bCREB, whereas overexpression of cATF2 induced NED. Last, stable expression of CREB-S133A or nATF2 inhibited IR-induced NED.

The transcriptional regulation of cAMP responsive element–containing genes by ATF2 and CREB is dependent on individual genes. For example, the insulin promoter contains one cAMP responsive element–binding site, and both ATF2 and CREB can bind it. However, ATF2 activates the transcription of insulin, whereas CREB inhibits it (31). In the present work, we also observed that overexpression of VP16-bCREB increased expression of endogenous CgA and NSE, whereas overexpression of nATF2 inhibited VP16-bCREB–induced expression of NSE, but not CgA. Likewise, knockdown of ATF2 or overexpression of cATF2 increased expression of NSE, but not CgA. These results support the notion that the effect of CREB and ATF2 on target gene transcription is dependent on gene context. Although VP16-bCREB can induce CgA and NSE expression (Fig. 3*B*), stable expression of nATF2, but not CREB-S133A, inhibited IR-induced expression of CgA and NSE (Fig. 4*D*). Despite the fact that the CREB-S133A–expressing stable cell line seems to have a basal level of CgA

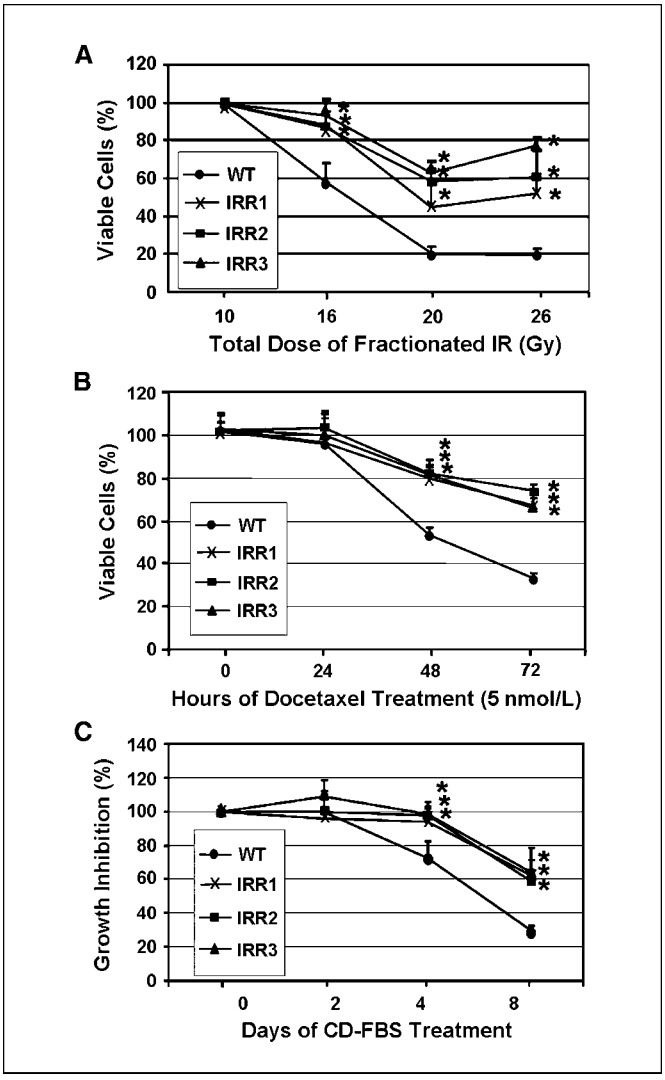

Figure 6. Cross-resistance of IR-resistant clones to therapeutic treatments. *A,* wild-type LNCaP and the indicated IR-resistant clones were cultured in 48-well plates and subjected to fractionated IR for the indicated doses. Cell viability was determined 1 d after the indicated irradiation as the percentage of viable cells that received 10-Gy irradiation. *B,* cells were treated with docetaxel for the indicated time and cell viability was determined as the percentage of viable cells at 0 h. *C,* cells were cultured in 10% FBS or CD-FBS for the indicated time and the inhibition of cell growth by CD-FBS was determined as described in Materials and Methods. *, $P < 0.01$, compared with wild-type LNCaP cells.

expression in the absence of tetracycline, which is likely due to leaky expression of CREB-S133A, induction of CREB-S133A by tetracycline did not alter the CgA expression in response to IR (Fig. 4*D*). Given that overexpression of VP16-bCREB induced expression of both CgA and NSE (Fig. 3*B*), these observations suggest that CREB is not responsible for IR-induced CgA and NSE expression. Alternatively, phosphorylation of CREB at different sites (21) may contribute to IR-induced CgA and NSE expression. Future studies are needed to distinguish these two possibilities. Interestingly, overexpression of CREB-S133A and nATF2 did not inhibit the growth of shorter neurites but rather inhibited the elongation of neurites (Fig. 4*C*). Consistent with a role of CREB in neurite elongation in hippocampal neurons (49), it is likely that CREB and ATF2 may oppose each other in irradiated LNCaP cells to regulate transcription of target genes essential for neurite elongation, one of the phases during neuritogenesis (50). Further identification of the target genes will provide insight into the molecular mechanisms by which CREB and ATF2 play opposing roles in IR-induced NED. Because expression of nATF2 inhibited IR-induced phosphoryaltion of CREB (Supplementary Fig. S3), it is possible that nuclear ATF2 may also antagonize an upstream signaling pathway that contributes to IR-induced phosphorylation of CREB. It will be interesting to determine whether this effect is independent of or dependent on ATF2 transcriptional activity. In addition, identification of cell signaling that regulates cytoplasmic accumulation of ATF2 and phosphorylation of CREB will provide opportunities to develop novel therapeutics for prostate cancer.

The finding that IR can induce NED is clinically important, given that ~10% to 60% of patients treated with radiation therapy experience recurrent tumors (2). Although a detailed and well-controlled examination of NE-like cells in recurrent tumors would shed light on our *in vitro* findings here, the fact that patients who have biochemical recurrence after radiotherapy normally do not undergo surgery or even biopsy prevents us from performing this type of study. In addition, the transient nature of NE-like cells may also not allow us to find a causative link between radiation therapy and the induction of NED in patients. We are therefore currently performing longitudinal analyses to evaluate the effect of radiation therapy on NED and its contribution to tumor recurrence in xenograft nude mouse prostate cancer models.

Disclosure of Potential Conflicts of Interest

No potential conflicts of interest were disclosed.

Acknowledgments

Received 6/12/2008; revised 8/18/2008; accepted 9/18/2008.

Grant support: Purdue Cancer Center Small Grants Program and the U.S. Army Medical Research Acquisition Activity, Prostate Cancer Research Program grant PC073098. DNA sequencing was done in Purdue Genomic Core Facility supported by National Cancer Institute grant CCSG CA23168 to the Purdue Cancer Center.

The costs of publication of this article were defrayed in part by the payment of page charges. This article must therefore be hereby marked *advertisement* in accordance with 18 U.S.C. Section 1734 solely to indicate this fact.

We thank Drs. Robert Geahlen, David Riese, Jian Jian Li, and Timothy Ratliff for their support and consultation during the course of this work, and the members of the Hu laboratory for helpful discussions.

References

1. Ganswindt U, Paulsen F, Anastasiadis AG, Stenzl A, Bamberg M, Belka C. 70 Gy or more: which dose for which prostate cancer? J Cancer Res Clin Oncol 2005;131:407–19.
2. Allen GW, Howard AR, Jarrard DF, Ritter MA. Management of prostate cancer recurrences after radiation therapy-brachytherapy as a salvage option. Cancer 2007;110:1405–16.
3. Daneshmand S, Quek ML, Pinski J. Neuroendocrine differentiation in prostate cancer. Cancer Ther 2005;3:383–96.
4. Nelson EC, Cambio AJ, Yang JC, Ok JH, Lara PN, Jr., Evans CP. Clinical implications of neuroendocrine differentiation in prostate cancer. Prostate Cancer Prostatic Dis 2007;10:6–14.
5. Amorino GP, Parsons SJ. Neuroendocrine cells in prostate cancer. Crit Rev Eukaryot Gene Expr 2004;14:287–300.
6. Yuan TC, Veeramani S, Lin MF. Neuroendocrine-like prostate cancer cells: neuroendocrine transdifferentiation of prostate adenocarcinoma cells. Endocr Relat Cancer 2007;14:531–47.
7. Deeble PD, Cox ME, Frierson HF, Jr., et al. Androgen-independent growth and tumorigenesis of prostate cancer cells are enhanced by the presence of PKA-differentiated neuroendocrine cells. Cancer Res 2007;67:3663–72.
8. Nakada SY, di Sant'Agnese PA, Moynes RA, et al. The androgen receptor status of neuroendocrine cells in human benign and malignant prostatic tissue. Cancer Res 1993;53:1967–70.
9. Bonkhoff H. Neuroendocrine differentiation in human prostate cancer. Morphogenesis, proliferation and androgen receptor status. Ann Oncol 2001;12 Suppl 2:S141–4.
10. Fixemer T, Remberger K, Bonkhoff H. Apoptosis resistance of neuroendocrine phenotypes in prostatic adenocarcinoma. Prostate 2002;53:118–23.
11. Vanoverberghe K, Vanden Abeele F, Mariot P, et al. Ca^{2+} homeostasis and apoptotic resistance of neuroendocrine-differentiated prostate cancer cells. Cell Death Differ 2004;11:321–30.
12. Cox ME, Deeble PD, Lakhani S, Parsons SJ. Acquisition of neuroendocrine characteristics by prostate tumor cells is reversible: implications for prostate cancer progression. Cancer Res 1999;59:3821–30.
13. Mayr B, Montminy M. Transcriptional regulation by the phosphorylation-dependent factor CREB. Nat Rev Mol Cell Biol 2001;2:599–609.
14. Brindle PK, Montminy MR. The CREB family of transcription activators. Curr Opin Genet Dev 1992;2:199–204.
15. Shaywitz AJ, Greenberg ME. CREB: a stimulus-induced transcription factor activated by a diverse array of extracellular signals. Annu Rev Biochem 1999;68:821–61.
16. Montminy MR, Bilezikjian LM. Binding of a nuclear protein to the cyclic-AMP response element of the somatostatin gene. Nature 1987;328:175–8.
17. Garcia GE, Nicole A, Bhaskaran S, Gupta A, Kyprianou N, Kumar AP. Akt-and CREB-mediated prostate cancer cell proliferation inhibition by Nexrutine, a Phellodendron amurense extract. Neoplasia 2006;8:523–33.
18. Unni E, Sun S, Nan B, et al. Changes in androgen receptor nongenotropic signaling correlate with transition of LNCaP cells to androgen independence. Cancer Res 2004;64:7156–68.
19. Canaff L, Bevan S, Wheeler DG, et al. Analysis of molecular mechanisms controlling neuroendocrine cell specific transcription of the chromogranin A gene. Endocrinology 1998;139:1184–96.
20. Kim J, Jia L, Stallcup MR, Coetzee GA. The role of protein kinase A pathway and cAMP responsive element-binding protein in androgen receptor-mediated transcription at the prostate-specific antigen locus. J Mol Endocrinol 2005;34:107–18.
21. Johannessen M, Moens U. Multisite phosphorylation of the cAMP response element-binding protein (CREB) by a diversity of protein kinases. Front Biosci 2007;12:1814–32.
22. Hai TW, Liu F, Coukos WJ, Green MR. Transcription factor ATF cDNA clones: an extensive family of leucine zipper proteins able to selectively form DNA-binding heterodimers. Genes Dev 1989;3:2083–90.
23. Maekawa T, Sakura H, Kanei-Ishii C, et al. Leucine zipper structure of the protein CRE-BP1 binding to the cyclic AMP response element in brain. EMBO J 1989;8:2023–8.
24. Wagner EF. AP-1-Introductory remarks. Oncogene 2001;20:2334–5.
25. Eferl R, Wagner EF. AP-1: a double-edged sword in tumorigenesis. Nat Rev Cancer 2003;3:859–68.
26. Gueorguiev VD, Cheng SY, Sabban EL. Prolonged activation of cAMP-response element-binding protein and ATF-2 needed for nicotine-triggered elevation of tyrosine hydroxylase gene transcription in PC12 cells. J Biol Chem 2006;281:10188–95.
27. Ionescu AM, Drissi H, Schwarz EM, et al. CREB Cooperates with BMP-stimulated Smad signaling to enhance transcription of the Smad6 promoter. J Cell Physiol 2004;198:428–40.
28. Ionescu AM, Schwarz EM, Zuscik MJ, et al. ATF-2 cooperates with Smad3 to mediate TGF-β effects on chondrocyte maturation. Exp Cell Res 2003;288:198–207.
29. Niwano K, Arai M, Koitabashi N, et al. Competitive binding of CREB and ATF2 to cAMP/ATF responsive element regulates eNOS gene expression in endothelial cells. Arterioscler Thromb Vasc Biol 2006;26:1036–42.
30. Flint KJ, Jones NC. Differential regulation of three members of the ATF/CREB family of DNA-binding proteins. Oncogene 1991;6:2019–26.
31. Hay CW, Ferguson LA, Docherty K. ATF-2 stimulates the human insulin promoter through the conserved CRE2 sequence. Biochim Biophys Acta 2007;1769:79–91.
32. Ricote M, Garcia-Tunon I, Bethencourt F, et al. The p38 transduction pathway in prostatic neoplasia. J Pathol 2006;208:401–7.

33. Liu H, Deng X, Shyu YJ, Li JJ, Taparowsky EJ, Hu CD. Mutual regulation of c-Jun and ATF2 by transcriptional activation and subcellular localization. EMBO J 2006;25: 1058–69.

34. Paulmurugan R, Gambhir SS. Firefly luciferase enzyme fragment complementation for imaging in cells and living animals. Anal Chem 2005;77:1295–302.

35. Kudo N, Wolff B, Sekimoto T, et al. Leptomycin B inhibition of signal-mediated nuclear export by direct binding to CRM1. Exp Cell Res 1998;242:540–7.

36. Reusch JE, Colton LA, Klemm DJ. CREB activation induces adipogenesis in 3T3-1 cells. Mol Cell Biol 2000; 20:1008–20.

37. Barco A, Alarcon JM, Kandel ER. Expression of constitutively active CREB protein facilitates the late phase of long-term potentiation by enhancing synaptic capture. Cell 2002;108:689–703.

38. de Wit R. Chemotherapy in hormone-refractory prostate cancer. BJU Int 2008;101 Suppl 2:11–5.

39. di Sant'Agnese PA. Neuroendocrine differentiation in prostatic carcinoma: an update on recent developments. Ann Oncol 2001;12 Suppl 2:S135–40.

40. Huang J, Wu C, di Sant'Agnese PA, Yao JL, Cheng L, Na Y. Function and molecular mechanisms of neuroendocrine cells in prostate cancer. Anal Quant Cytol Histol 2007;29:128–38.

41. Yuan TC, Veeramani S, Lin FF, et al. Androgen deprivation induces human prostate epithelial neuroendocrine differentiation of androgen-sensitive LNCaP cells. Endocr Relat Cancer 2006;13:151–67.

42. Ismail AH, Landry F, Aprikian AG, Chevalier S. Androgen ablation promotes neuroendocrine cell differentiation in dog and human prostate. Prostate 2002; 51:117–25.

43. Wright ME, Tsai MJ, Aebersold R. Androgen receptor represses the neuroendocrine transdifferentiation process in prostate cancer cells. Mol Endocrinol 2003;17: 1726–37.

44. Jin RJ, Wang Y, Masumori N, et al. NE-10 neuroendocrine cancer promotes the LNCaP xenograft growth in castrated mice. Cancer Res 2004;64:5489–95.

45. Jiborn T, Bjartell A, Abrahamsson PA. Neuroendocrine differentiation in prostatic carcinoma during hormonal treatment. Urology 1998;51:585–9.

46. Zhang XQ, Kondrikov D, Yuan TC, Lin FF, Hansen J, Lin MF. Receptor protein tyrosine phosphatase α signaling is involved in androgen depletion–induced neuroendocrine differentiation of androgen-sensitive LNCaP human prostate cancer cells. Oncogene 2003; 22:6704–16.

47. Spiotto MT, Chung TD. STAT3 mediates IL-6-induced neuroendocrine differentiation in prostate cancer cells. Prostate 2000;42:186–95.

48. Yang X, Chen MW, Terry S, et al. A human- and male-specific protocadherin that acts through the wnt signaling pathway to induce neuroendocrine transdifferentiation of prostate cancer cells. Cancer Res 2005;65:5263–71.

49. Karasewski L, Ferreira A. MAPK signal transduction pathway mediates agrin effects on neurite elongation in cultured hippocampal neurons. J Neurobiol 2003;55: 14–24.

50. Aletta JM, Greene LA. Growth cone configuration and advance: a time-lapse study using video-enhanced differential interference contrast microscopy. J Neurosci 1988;8:1425–35.

Legends to Supplementary Figures

Supplementary SFig. 1. **IR induces cytoplasmic accumulation of ATF2 and nuclear accumulation of pCREB in NE-like cells.** (*A*). LNCaP cells cultured in 10 cm dishes were irradiated with fractionated IR (2 Gy/day, 5 days/week) for four weeks to induce NE-like differentiation. Subcellular localization of ATF2 in NE-like cells was determined using immunostaining. DAPI staining was used to mark the nucleus. Subcellular localization of ATF2 in proliferating LNCaP cells was shown in Fig. 2A. (*B*). LNCaP cells were similarly treated as described in (*A*) and cytosolic and nuclear extracts were prepared. For the purpose of comparison, non-irradiated cells (-) and cells that received 5 times of exposure to IR (10 Gy) were also included. Note that only 10 μg of cytosolic extract and the equal portion of nuclear extract were loaded for immunoblotting of pCREB.

Supplementary SFig. 2 ATF2 and CREB play an opposing role in NE-like differentiation. Shown are representative images acquired from cells transfected with plasmids encoding the indicated siRNA constructs (*A*), mutant CREB (*B*), or mutant ATF2 (*C*) as presented in Fig. 3. (*D*) Shown are subcellular localization of cATF2 and nATF2 as Venus fusions.

Supplementary SFig. 3. Effect of nATF2 on IR-induced phosphorylation of CREB. The LNCaP cells that stably express inducible nATF2 were cultured in 10 cm dishes and subjected to IR (2 Gy/day) for five days while nATF2 expression was constantly induced by tetracycline (Tet +) or not induced (Tet -). Irradiated cells were harvested, and

cytosolic (C) and nuclear (N) fractions were prepared. The amount of pCREB, CREB, and ATF2 in the cytosolic and nuclear fractions was determined using immunoblotting.

Supplementary SFig. 4. Morphology of wild-type LNCaP (WT) and the indicated isolated IR-resistant clones from dedifferentiated NE-like cells.

Supplementary SFig. 5. IR- and androgen depletion-induced NE-like morphological changes in wild-type LNCaP (WT) cells and IR-resistant clones. (*A*) Shown are representative images of irradiated cells acquired at the end of 40 Gy-irradiation. (*B*) Shown are representative images of cells acquired at the end of three-week treatment with C/D-FBS.

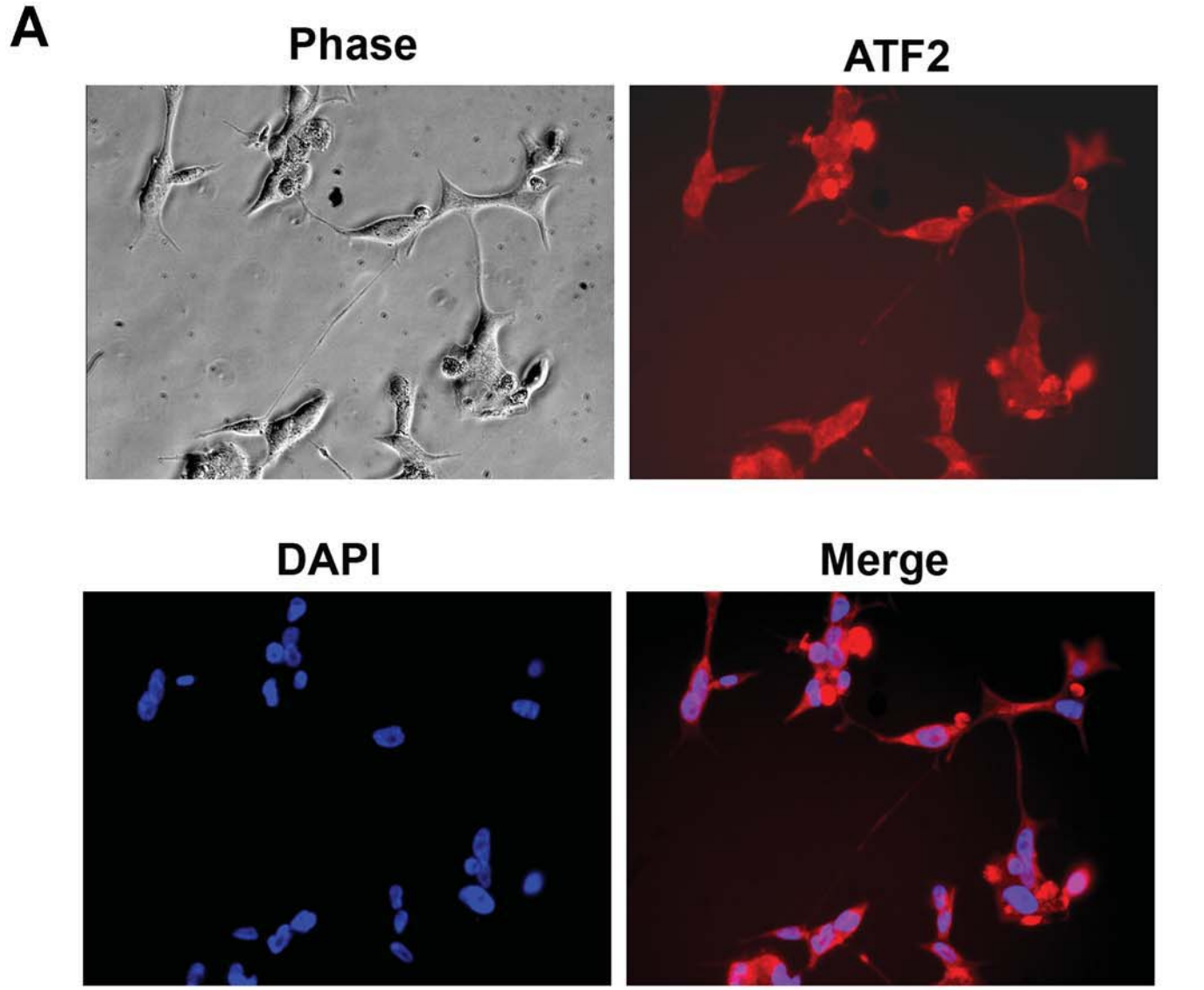
A
Phase
ATF2
DAPI
Merge
B
–
10 Gy
40 Gy
C
N
C
N
C
N
pCREB
Histone 3
β–tubulin

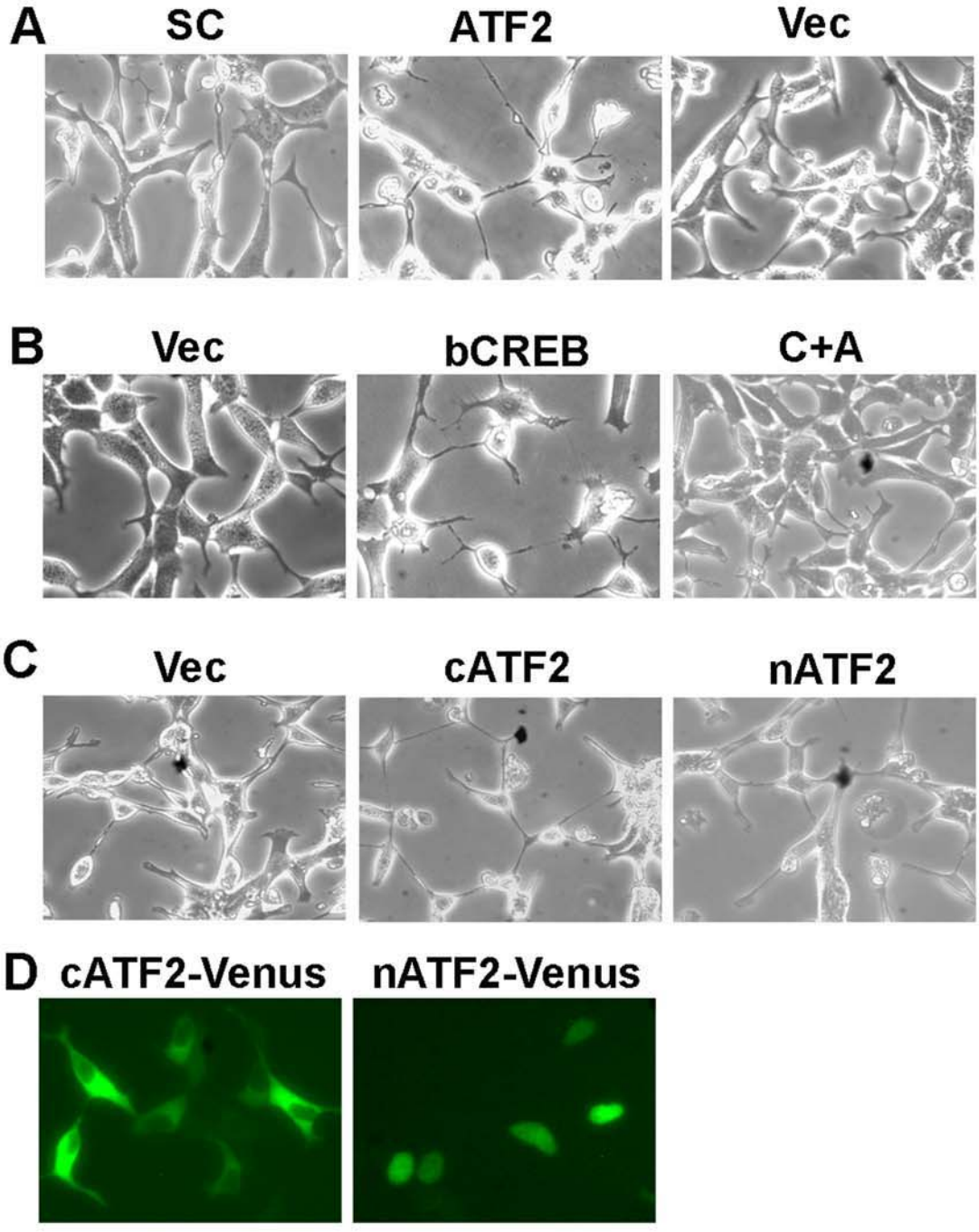
A
SC
ATF2
Vec
B
Vec
bCREB
C+A
C
Vec
cATF2
nATF2
D
cATF2-Venus
nATF2-Venus

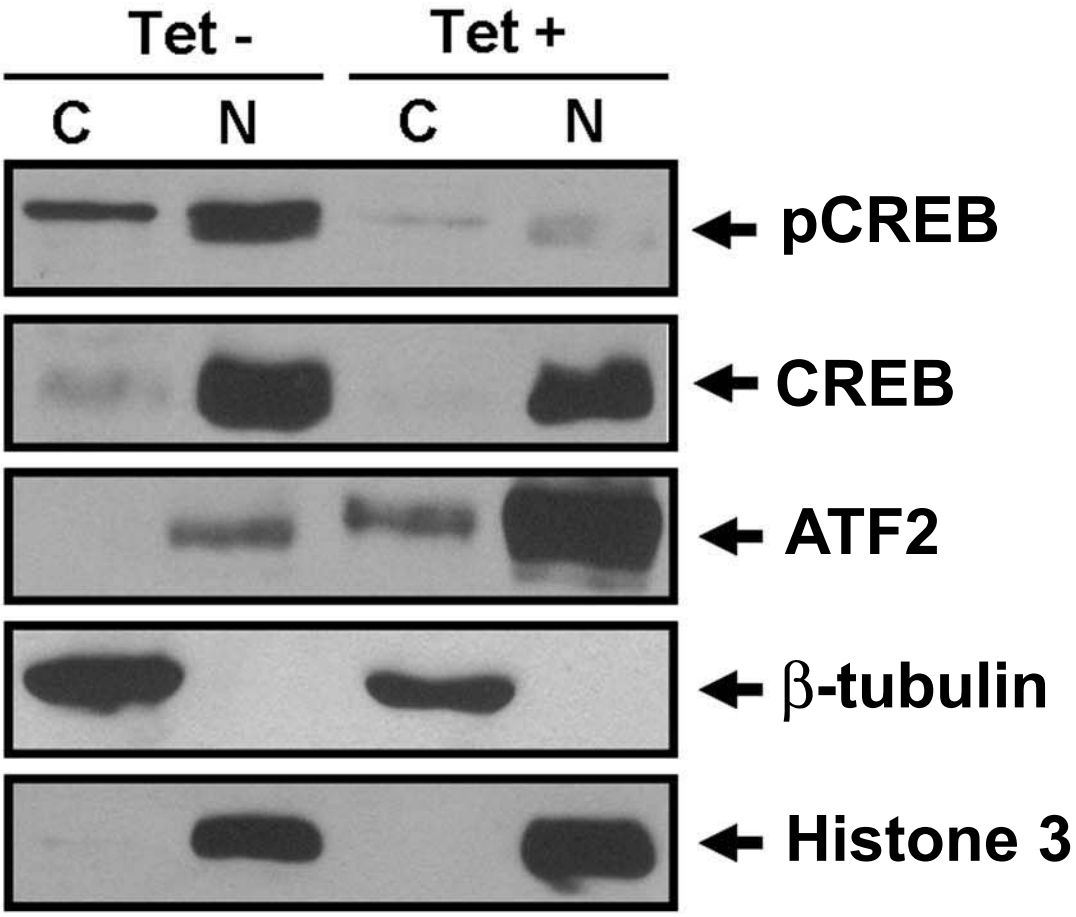
Tet -
Tet +
C
N
C
N
pCREB
CREB
ATF2
β-tubulin
Histone 3

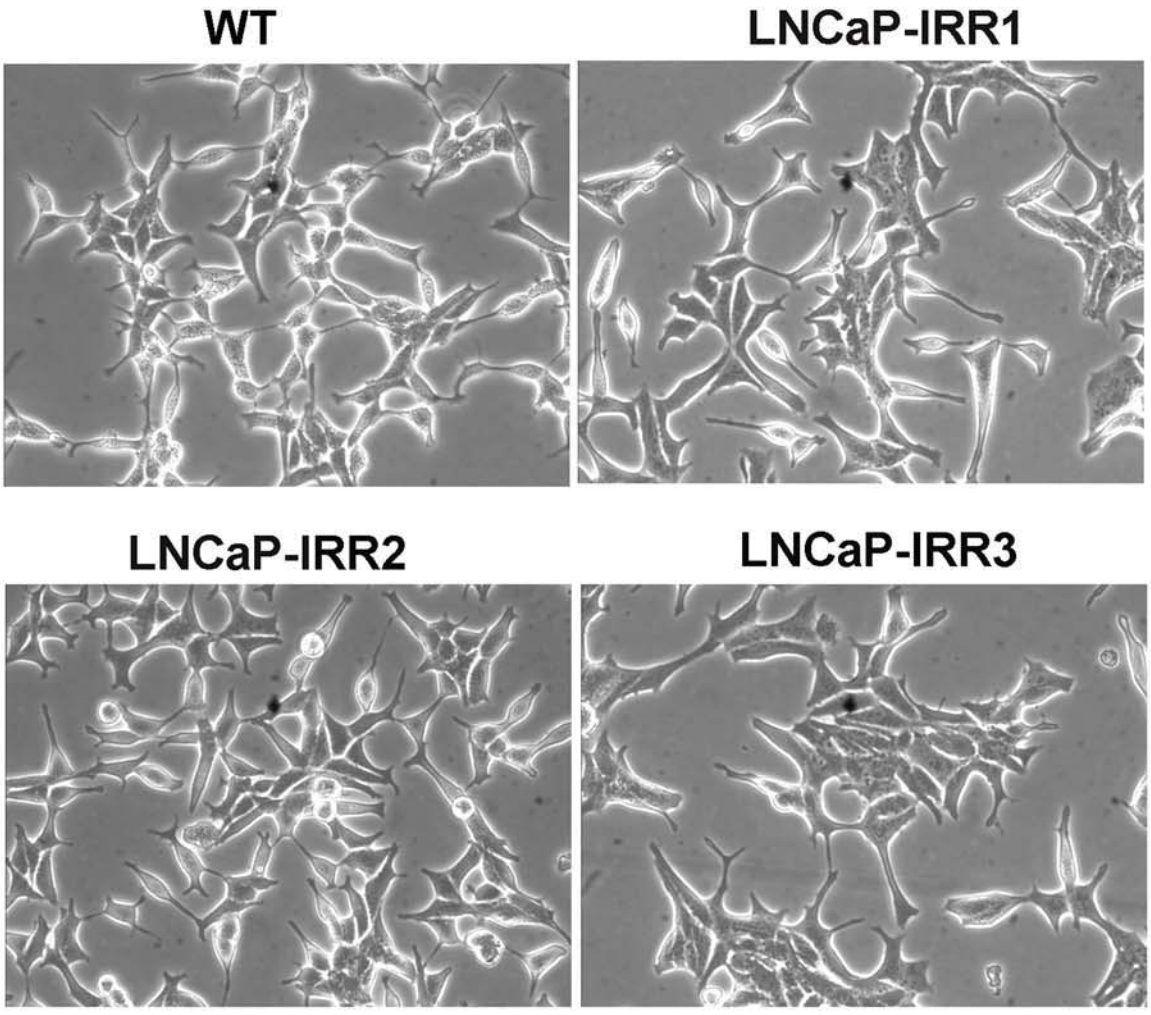
WT
LNCaP-IRR1
LNCaP-IRR2
LNCaP-IRR3

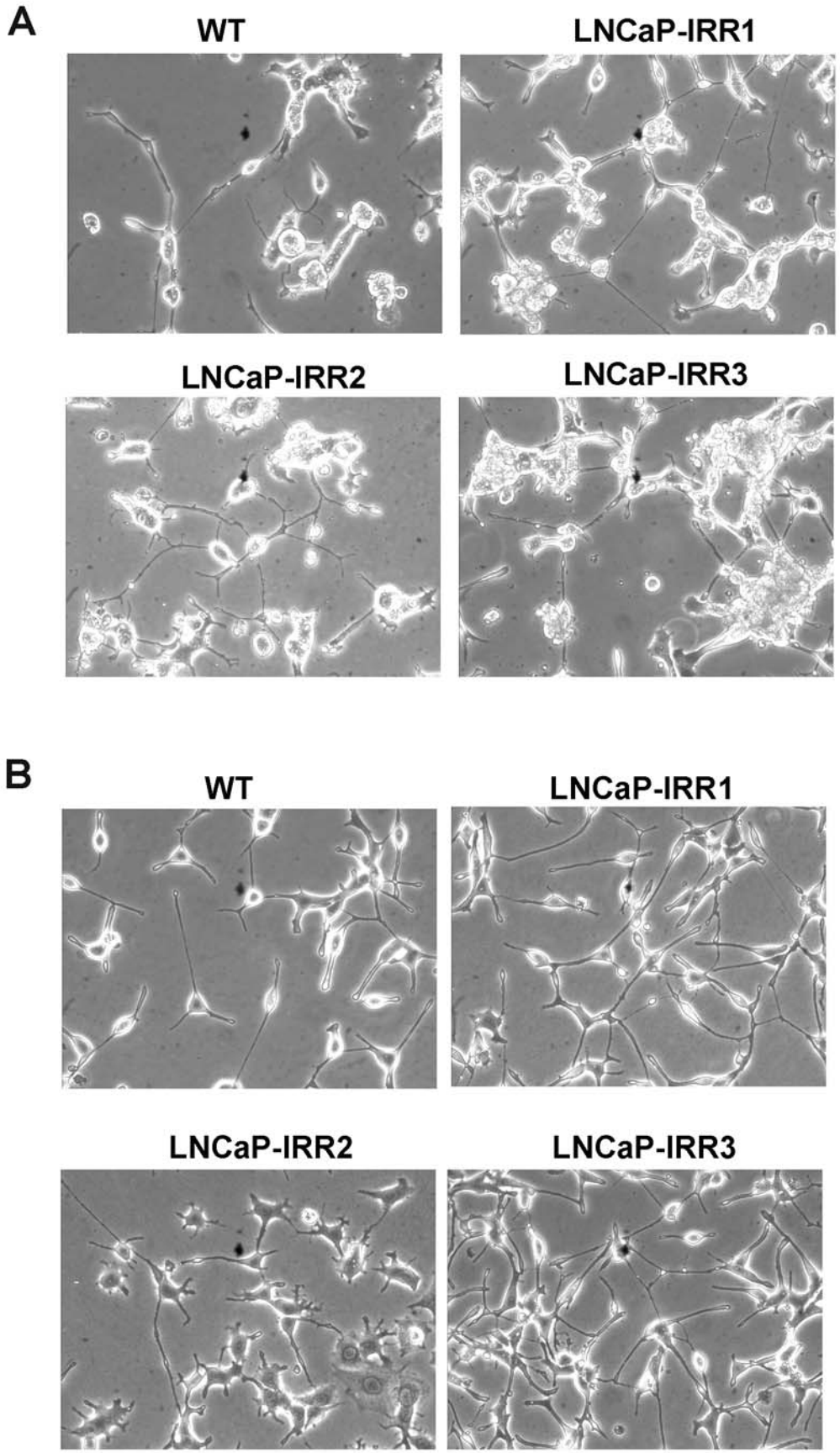
A
WT
LNCaP-IRR1
LNCaP-IRR2
LNCaP-IRR3
B
WT
LNCaP-IRR1
LNCaP-IRR2
LNCaP-IRR3

Ionizing radiation induces neuroendocrine differentiation in prostate cancer cells *in vitro, in vivo* and in prostate cancer patients

Xuehong Deng[1], Bennett D. Elzey[1], Jeanine M. Poulson[3], Wallace B. Morrison[3], Song-Chu Ko[4], Noah M. Hahn[5], Timothy L. Ratliff[2], and Chang-Deng Hu[1, *]

[1]Department of Medicinal Chemistry, [2]Department of Comparative Pathobiology, and [3]Department of Clinical Veterinary Science[3], Purdue University, West Lafayette, IN 47907, USA; [4]Department of Radiation Oncology and [4]Department of Medicine, Indiana University School of Medicine, Indianapolis, IN 46202, USA.

* To whom correspondence should be addressed; Email: hu1@purdue.edu; Tel: 1-765-496-1971; Fax: 1-765-494-1414

Emails for coauthors:

X. Deng: deng1@purdue.edu

B.D. Elzey: belzey@iupui.edu

J.M. Poulson: jpoulson@purdue.edu

W.B. Morrison: wbm@purdue.edu

S.C. Ko: soko@iupui.edu

N.M. Hahn: nhahn@iupui.edu

T.L. Ratliff: tlratliff@purdue.edu

Running Title: IR induces neuroendocrine differentiation in prostate cancer cells

Abstract

Prostate cancer remains the most common noncutaneous cancer among American men. Although most patients can be cured by surgery and radiotherapy, 32,050 patients still died of the disease in 2010. Because most prostate cancer patients initially present as localized cancer, they were likely treated with radiotherapy either as a primary therapy, salvage therapy, or in combination with surgery or hormonal therapy. Despite the efficacy of radiotherapy, several studies suggest that approximately 10% and up to 30-60% of prostate cancer patients experience biochemical recurrence within five years after radiotherapy. Thus, elucidating the molecular mechanisms underlying radioresistance and tumor recurrence will likely have a significant impact on prostate cancer mortality. We previously demonstrated that fractionated ionizing radiation (IR) can induce prostate cancer cells LNCaP to undergo neuroendocrine differentiation (NED) by activation of cAMP response element binding protein (CREB) and cytoplasmic sequestration of ATF2, two CRE-binding transcription factors that oppose each other to regulate NED. Importantly, IR-induced NED is reversible and de-differentiated cells are cross-resistant to IR, androgen depletion and docetaxel treatments. These findings suggest that radiation-induced NED may allow prostate cancer cells to survive treatment and contribute to tumor recurrence. In the present study, we further demonstrated that IR also induces NED in a subset of DU-145 and PC-3 cells. In addition, we confirmed that IR induces NED in LNCaP xenograft tumors in nude mice, and observed that the plasma chromogranin A (CgA) level, a biomarker for NED, is increased by 2- to 4-fold in tumor-bearing mice after 20 and 40 Gy of irradiation, respectively. Consistent with these *in vivo* findings, a pilot study in prostate cancer patients showed that the serum CgA level is elevated in 4 out of 9 patients after radiotherapy. Taken together, these findings provide evidence that radiation-induced NED is a general therapeutic response in a

subset of prostate cancer patients. Thus, a large scale analysis of radiotherapy-induced NED in prostate cancer patients and its correlation to clinical outcomes will likely provide new insight into the role of NED in prostate cancer radiotherapy and the prognosis.

Key words: Ionizing radiation, prostate cancer, neuroendocrine differentiation, ATF2, CREB, radiotherapy

Introduction

Prostate cancer is the second leading cause of cancer death in men in the US [1]. Despite the progress over the last two decades, the only curative treatments for localized prostate cancer are surgery and radiotherapy (RT). Although most patients can be cured, several large scale studies suggest that 10% of patients with low-risk prostate cancer and up to 30-60% of patients with high-risk prostate cancer experienced biochemical recurrence within 5 years after RT, among them 20-30% died within 10 years [2-6]. Given that only 2.4% of prostate cancer patients in the US initially present as bone metastasis, which can only be temporally controlled by non-curative hormonal therapy, the majority of deaths were from those who went through the primary treatment of localized cancer, local recurrence, salvage therapy, and eventually distant recurrence, hormonal therapy, and death. Because RT is one of the primary treatments for low-risk localized prostate cancer, a major treatment for high-risk prostate cancer when combined with hormonal therapy, a major salvage therapy for local recurrence, and a recommended adjuvant therapy for patients undergoing surgery [7-13], enhancing the sensitivity of prostate cancer cells to RT will likely reduce, or even prevent, tumor recurrence and impact the management of advanced prostate cancer.

The prostate gland constitutes three types of epithelial cells including luminal, basal and neuroendocrine cells. While luminal and basal cells are the majority of the prostatic epithelial cells, NE cells are less than 1% of total epithelial cells. Although the physiological role of NE cells remains to be investigated, increased number of NE-like cells is observed in advanced prostate cancer patients [14, 15]. NE-like cells are androgen receptor (AR) negative and they do not proliferate [16]. However, NE-like cells secret a number of peptide hormones and growth factors to support the growth of surrounding tumor cells [17]. In addition, NE-like cells are

reversible and can de-differentiate back to a proliferating state, which may contribute to tumor recurrence [18, 19]. Further, NE-like cells express high levels of Bcl-2 and are highly apoptosis resistant [7, 20, 21]. Because the quantification of NED by identifying chromogranin A (CgA) or neuron specific enolase (NSE) positive cells from prostate cancer tissues is affected by several factors such as location of sampling and tumor volume, controversial results regarding the clinical correlation of NED to disease progression have been reported [15, 17, 22-25]. To overcome this challenge, several studies measured serum biomarkers of NED and demonstrated that the serum CgA level is the best biomarker to reflect the extent of NED in prostate cancer tissues [26-28]. Importantly, an increase in the serum CgA level correlates with disease progression and the acquisition of castration-resistant prostate cancer [25, 27, 29-32], suggesting that NED may represent a novel mechanism by which prostate cancer cells survive treatment and contribute to recurrence. Thus, targeting NE-like cells has recently been proposed and developed to treat prostate cancer [7, 8, 14, 17, 22, 33].

A number of stimuli, such as cAMP [18, 34-36], IL-6 [23, 36-42], androgen ablation therapy [43-48], and EGF [21], have been reported to induce prostate cancer cells to undergo NED. We recently observed that the prostate cancer LNCaP cells also underwent NED after receiving clinically relevant dose of fractionated ionizing radiation (IR) [19]. Upon IR for four weeks, the remaining survival cells (~20%) all differentiated into NE-like cells and expressed higher levels of CgA and NSE [19]. In addition, IR-induced NE-like cells also expressed higher levels of synaptophysin and prostatic acid phosphatase, but lower level of PSA and AR (unpublished results). Furthermore, we observed that two transcription factors cAMP response element binding protein (CREB) and activating transcription factor 2 (ATF2) oppose each other to regulate NED. Consistent with this notion, IR induced cytoplasmic sequestration of ATF2 and

increased phosphorylation of nuclear CREB. In the present study, we extend these findings to two other prostate cancer cell lines, and provide evidence that radiation also induces NED in LNCaP xenograft tumors in nude mice and in human prostate cancer patients.

Materials and Methods

Cell culture and analysis of NED: Cell culture and NED analysis were exactly the same as previously reported [19] except that LNCaP cells were cultured in RPMI1640, and DU-145 in MEM, and PC-3 cells in F-12K media. The radiation protocol, VP16-bCREB, and ATF2 shRNAs used in the present work to determine the effect of IR, VP16-bCREB and ATF2 knockdown on NED in DU-145 and PC-3 cells were also described before [19]. Likewise, immunofluorescence and subcellular fractionation methods were similarly used to determine the effect of IR on the phosphorylation of CREB and subcellular localization of ATF2.

IR-induced NED in xenograft tumors in nude mice: The LNCaP human prostate cancer cells were implanted subcutaneously by injecting $5x10^6$ cells 1:1 in Matrigel into the thighs of 6-week old male athymic nude mice (BALB/c strain). When tumors reached 300-500 mm^3, tumors were subjected to X-ray irradiation (5 Gy/fraction) twice a week for a total dose of 40 Gy or the indicated doses using a Linear Accelerator (6 MV) in the Linda and William Fleischhauer Radiation Facility at Purdue University. Tumor volumes were measured twice a week or during blood sample collections. For immunohistochemical (IHC) analysis of NED in xenograft tumors, tumors were resected at the end of 40 Gy treatment, and formalin fixed and paraffin embedded. Tissue slides were prepared at 5 μm thickness, and CgA was stained by the anti-CgA (Abcam). To determine the effect of X-ray irradiation on plasma CgA and PSA levels, vein blood samples were drawn before the beginning of treatment (0 Gy), the end of 2-week (20 Gy) and 4-week (40 Gy) treatment, and plasma was used for measuring plasma CgA and PSA using the CgA EIA kit (Cosmo Bio) and the PSA ELISA Kit (Calbiotech) according to manufacturer's instructions. Plasma CgA levels were normalized to tumor volume or plasma PSA levels, and fold change was determined with compared with 0 Gy time point. For control mice, 0 time point was designated

when xenograft tumors reached 300-500 mm^3, and blood was drawn for 0 Gy time point. After that, two blood collections for week 2 and 4 time points (equivalent to 20 Gy and 40 Gy in irradiated mice group) were conducted at the end of 2 and 4 weeks, respectively. All animal experiments were approved by the Purdue Animal Care and Use (PACUC No. 08-127), and all animal cares followed the Assurance of Compliance with Public Health Services Policy on Human Care and Use of Laboratory Animals (Welfare Assurance #A3231-01).

Serum CgA and PSA measurement in human prostate cancer patients. Nine patients diagnosed with localized prostate cancer (six T1c and one of each T2b, T2c, and T3a) were enrolled at Indiana University School of Medicine. All patients signed the consent form and agreed to participate in the pilot study according to the approved Institutional Research Board protocol (0805-43). The average age of patients was 54.6 years old. Five patients had a Gleason score 7, one patient 9, and three patients 6. All patients were treated at the Midwest Proton Radiotherapy Institute with the total dose of 72 Gy delivered. To determine the effect of RT on serum CgA levels, three blood samples were drawn before the start of RT treatment, in the middle of the treatment (week 4-5), and after the treatment (end of week 7), designated Before, Middle and After, respectively. Serum CgA and PSA levels were measured using the CgA EIA kit (Cosmo Bio) and the PSA ELISA Kit (Calbiotech) according to the manufacturer's instruction. Because some prostate cancer patients maintain a high level of serum CgA, which is likely determined by the number of pre-existing NE-like cells and cancer cells that secrete CgA, serum CgA levels were normalized to serum PSA levels for the calculation of fold increase.

Results

IR induces morphological changes and expression of NE markers to various extents in prostate cancer cells. To know whether our findings with LNCaP cells can be extended to other prostate cancer cells, we performed similar experiments in DU-15 and PC-3 cells as we did with LNCaP cells [19]. In LNCaP cells, cell bodies became smaller and almost all cells were connected via longer neurites. In contrast, enlarged cell bodies were observed for both DU-145 and PC-3 cells. Unlike LNCaP cells in which almost all survived cells showed extended neurites, only a subset of irradiated DU-145 cells (32%) showed neurite outgrowth whereas non-irradiated DU-145 cells did not show any neurite outgrowth (Fig. 1A). Interestingly, approximately 6% of non-irradiated PC-3 cells already displayed neurite outgrowth whereas IR increased the number of cells with neurite outgrowth to 35%. Consistent with the morphological changes, NSE was also induced in DU-145 and PC-3, albeit to a lesser extent when compared with LNCaP cells. However, no significant induction of CgA in DU-145 and PC-3 was observed when compared with LNCaP cells. While these results confirm that IR can induce DU-145 and PC-3 cells to differentiate into NE-like cells, they also suggest that a subset of DU-145 and PC-3 cells is refractory to IR. This is also consistent with the differential responses of prostate cancer cell lines to androgen depletion, IL-6, cAMP and EGF treatments [21, 23].

Effect of IR on CREB activation and ATF2 subcellar localization. In LNCaP cells, we observed that IR-induced NED is associated with increased nuclear phospho-CREB and cytoplasmic-localized ATF2. To know whether IR also activates CREB and induces cytolasmic localization of ATF2 in these cell lines, we performed immunofluorescece analysis and subcellular fraction. We observed that CREB was highly phosphorylated in irradiated DU-145, but to a lesser extent in PC-3 (Fig. 2A). Interestingly, increased cytoplasmic localization of

ATF2 was observed in both DU-145 and PC-3 cells (Fig. 2B). However, only a subset of cells (~50%) showed cytoplasmic localization of ATF2 in these two cell lines, whereas increased cytoplasmic localization was observed in almost all irradiated LNCaP cells. Consistent with immunofluorescence analysis, subcellular fractionation also showed only a slight increase of ATF2 in the cytosolic fraction in irradiated DU-145 and PC-3 cells, which is likely due to increased cytoplasmic localization of ATF2 in a subset of cells (data not shown). Thus, we conclude that IR can similarly induce CREB activation and impair ATF2 nuclear localization in a subset of DU-145 and PC-3 cells.

Overexpression of VP16-bCREB or ATF2 knockdown induces NED in DU-145 and PC-3 cells. The above results suggest that DU-145 and PC-3 cell may have intrinsic defects in activating CREB or sequestering ATF2 in the cytoplasm in some cells. To know whether these cells can be still induced by a constitutively activated CREB VP16-bCREB, we performed similar experiments in these two cell lines as we did in LNCaP cells [19]. We observed that overexpression of VP16-bCREB also induced neurite extension in a subset of DU-145 (14%) and PC-3 cells (21%) (Fig. 3A). Consistent with the morphological changes, a slight induction of both CgA and NSE was observed in DU-145 transfected with VP16-bCREB (Fig. 3C). However, only a slight induction of NSE, but not CgA, was observed in PC-3 cells transfected with VP16-CREB (Fig. 3B). Because the transfection efficiency is relatively low in these two cell lines, these results suggest that expression of VP16-bCREB also induced NED in DU-145 and PC-3 cells, at least in a subset of cells.

Similar results were obtained when ATF2 was knocked down in both DU-145 and PC-3 cells (Fig. 4). While no extended neurites were observed in DU-145 cells transfected with

scrambled control, approximately 25% of DU-145 transfected with the ATF2 shRNA plasmids for five days showed neurite outgrowth. Similarly, 26% of PC-3 cells transfected with ATF2 shRNA plasmids for five days showed neurite outgrowth whereas 4.5% of cells transfected with scrambled control plasmids showed neurite outgrowth.

Radiation induces NED in LNCaP xenograft tumors in nude mice. To determine whether IR can induce NED *in vivo*, we employed nude mouse xenograft models. For this purpose, we used LNCaP cells as they can be better induced by IR to undergo NED. LNCaP xenograft tumors were established by subcutaneous inoculation of LNCaP cells in hind legs in nude mice. When xenograft tumors grew to approximately 300-500 mm^3, we performed X-ray irradiation to xenograft tumors at 10 Gy/week (5 Gy/fraction). Our preliminary results with this irradiation protocol similarly induced NED *in vitro* (unpublished observation). Thus, this irradiation protocol avoided multiple anesthesia treatments to mice. At the end of four weeks, mice were sacrificed and residual tumor nodules were resected for IHC analysis of CgA expression. Compared to non-irradiated tumors (n=3), some cells in all irradiated tumors (n=10) showed higher expression of CgA, suggesting that radiation indeed induces NED in xenograft tumors (Fig. 5A).

Because serum/plasma CgA levels can be used to quantify the extent of NED in prostate cancer tissues in human patients, we next performed similar fractionated IR to xenograft tumors and measured the plasma CgA level. We collected blood samples before irradiation, at the end of 2 and 4 weeks of irradiation from tumor-bearing mice (n=10). As controls, blood samples from tumor-bearing mice (n=10) that did not receive radiation treatment were similarly collected at the corresponding time points (equivalent to 0, 2 and 4 weeks). Because higher plasma CgA levels were observed in all mice bearing large tumors without receiving irradiation, which is likely due

to the increased number of LNCaP cells that express basal levels of CgA, we normalized plasma CgA levels to plasma PSA levels. Three out of 10 mice showed elevated plasma CgA levels at the end of 2-week irradiation, and 7 mice showed elevated plasma CgA levels at the end of 4-week irradiation. In contrast, none of the non-irradiated tumor-bearing mice showed any elevation of plasma CgA levels at the corresponding time points. Instead, their normalized CgA levels were lower after 2-4 weeks of observation. Because these non-irradiated xenograft tumors continued to grow and reached 1300 mm^3 to 2300 mm^3 at the end of the corresponding 4-week time point, the lower normalized CgA levels in non-irradiated mice are likely due to overproduction of PSA in tumor cells. When plasma CgA levels in all 10 mice were considered, the average plasma CgA levels increased by 2- and 5-fold at the end of 2- and 4-week irradiation, respectively, whereas the average plasma CgA levels for control group decreased by 2-4 fold at the end of 2- to 4- weeks' observation, respectively (Fig. 5B). Thus, we conclude that X-ray irradiation can induce NED in xenograft tumors.

Prostate cancer patients show elevated levels of serum CgA after radiotherapy. Because serum CgA has been used as a biomarker to monitor hormonal therapy-induced NED in prostate cancer patients [25, 27, 29-32], the above observations that X-ray irradiation to xenograft tumors increased plasma CgA levels in nude mice prompted us to test if RT also induces serum CgA elevation in human prostate cancer patients. To this end, we collected blood samples before RT, in the middle of RT, and immediately after RT from prostate cancer patients enrolled at Indiana University School of Medicine, and measured serum CgA and PSA levels. Except for one patient from whom we missed the collection of his blood sample at the middle time point, we collected blood samples at all three time points from the other 8 patients. Among these 8 patients, 2

showed an increase in the serum CgA level at the middle of the RT treatment, and 6 patients showed a decrease in the serum CgA level. Interestingly, the CgA level at the end of the RT treatment in these 6 patients rebound to the pretreatment level or higher (Fig. 6). When compared with the CgA level before RT, 4 out of 9 patients showed 1.5-2.2 fold increase in serum CgA levels, 2 unchanged, and 2 a slight decrease (less than 2 fold) at the end of RT treatment. Thus, approximately 44% (4 out of 9) of patients showed serum CgA elevation after RT.

Discussion

Based on our recent findings that IR can induce NED in LNCaP cells, we provided evidence here that IR also induces NED in DU-145 and PC-3 cells albeit to a lesser extent. Consistent with this, IR treatment induced cytoplasmic localization of ATF2 and CREB phosphorylation in a subset of cells. Likewise, expression of a constitutively activated CREB or ATF2 knockdown also induced the expression of CgA and/or NSE, and neurite extension in these two cell lines. Thus, it is likely that radiation-induced NED is a general phenomenon. Furthermore, we have confirmed that IR also induced NED in LNCaP xenograft tumors in nude mice and that RT also induced elevation of serum CgA levels in 4 out of 9 prostate cancer patients. Our findings here together suggest that radiation-induced NED may represent a therapeutic response in a subset of prostate cancer patients undergoing radiotherapy.

Difference between LNCaP, DU-145 and PC-3 cells: The LNCaP cell line was established from a local metastasized lymph node whereas DU-145 and PC-3 were established from metastasized tumors in bone and brain, respectively [49]. Although the treatment history of these patients is not clear, it is possible that DU1-45 and PC-3 cells were established after extensive exposures to treatments. In addition, DU-145 and PC-3 cells do not express detectable levels of AR and other genetic, and possibly epigenetic, changes are involved. These intrinsic differences may be responsible for the differential induction of NED by other stimuli as well [23, 34]. Consistent with these observations, three clones isolated from regrowing cells after IR-induced NED are poorly responsive to IR and ADT [19]. Interestingly, we observed that CREB activation and ATF2 cytoplasmic sequestration only occurred in a subset of DU-145 and PC-3 cells after fractionated IR whereas almost all LNCaP cells after 10 Gy of irradiation showed increased pCREB in the nucleus and an increase of cytoplasmic localized ATF2. These observations

suggest that while DU-145 and PC-3 cells do contain a subset of cells that are inducible by IR to undergo NED, there are also some cells that are refractory to NED. Further analysis of these intrinsic differences among these three cell lines may shed new light on the molecular mechanisms underlying IR-induced NED.

CgA as a biomarker to monitor RT-induced NED. IHC staining of CgA and NSE has been widely used to identify NE-like cells in prostate cancer tissues. Because of the difficulty in quantifying NED using the IHC method, controversial results have been reported [15, 17, 22-25]. To resolve these controversies, several groups examined serum NE biomarkers and demonstrated that serum CgA is the best biomarker that can reflect NED in tissues [26-28]. In our xenograft nude mouse model, we not only observed increased numbers of tumor cells expressing higher levels of CgA in irradiated prostate xenograft tumors, but also observed an increase in the plasma CgA level in a dose-dependent manner in the majority of mice bearing irradiated xenograft tumors. In contrast, no increase in plasma CgA levels was observed in all tumor-bearing mice without receiving irradiation. Given the difficulty to perform biopsy in human prostate cancer patients undergoing RT, our results suggest that plasma or serum CgA levels can be used to monitor NED during treatment. In fact, results from a preliminary test with 9 prostate cancer patients suggest that RT increases serum CgA levels in about 44% of patients at the end of RT. It is worth noting that a previous study measured serum CgA and NSE levels in 100 prostate cancer patients before RT and three months after RT, and observed that 10 patients also showed elevated serum CgA levels three months after RT [50]. Since the number of prostate cancer cells has an impact on serum CgA levels, it is possible that many patients who underwent NED during treatment may eventually showed lower CgA levels due to the decrease in tumor cells. Because prostate cancer patients also often have pre-existing NE-like cells, it is therefore important to

monitor patient's response during RT by measuring serum CgA at multiple time points and compare with the serum CgA level before treatment. Indeed, we observed that 6 patients showed an initial decrease in serum CgA levels by the middle of RT, but rebound to the level comparable to or higher than that before RT. Because tumors start to shrink once treatment begins, an initial decrease in serum CgA levels and later rebound after the completion of the treatment may provide an interesting pattern to monitor RT-induced NED. Though one limitation of this pilot trial is the small sample size, the preliminary finding from this study warrants the necessity of a detailed analysis of RT-induced NED and its correlation to the clinical outcomes.

Can targeting NED be explored as a novel radiosensitization method? The extent of pre-existing NE-like cells and hormonal therapy-induced NED appear to contribute to disease progression and poor prognosis [25, 27, 29-32]. It is therefore proposed that targeting NED can be explored as a novel therapeutic approach [7, 8, 14, 17, 22, 33]. We have observed that CREB activation can be induced by IR as early as 10 Gy treatment in prostate cancer cells. In the case of LNCaP cells, approximately 80% of cells are killed by IR during the second week irradiation and the remaining 20% of cells survived the treatment undergo NED by the end of 4 weeks [19]. After that, no cell death occurred after continued irradiation up to 72 Gy. These observations suggest an interesting model that radiation-induced NED likely includes at least two important phases. The first phase is the selection and enrichment of radioresistant cells during the first two weeks, and the second phase is the NED phase during the second two weeks. Since increased CREB phoshphorylation was observed in a dose-dependent manner during the course of treatment, it is likely that CREB activation is not only involved in radioresistance but also involved in IR-induced NED. Thus, targeting CREB signaling in principle can sensitize prostate cancer cells to IR. In fact, targeting of CREB upstream signaling molecules such as PKA and

CaMKII in prostate cancer cells can induce cell death or sensitize cells to RT or ADT [51-54] [55, 56]. Because CREB can be phosphoryalted and activated by more than 15 different protein kinases such as MAPKs, AKT, PKA, CaMKII, ATM [57] and because many of these protein kinases can be activated by IR [58, 59], future identification of upstream protein kinases involved in radiation-induced CREB activation and NED may enable development of effective radiosensitizers for prostate cancer treatment.

Acknowledgements

We appreciate the input from the Hu lab, and we also thank Drs. Sarah Parson, Evan Keller, Jiaoti Huang, Liang Cheng, Peter Johnstone, and Michale Koch for the support and consultations during the course of this work. Thanks to Sandra Torregresa-Allen in the Molecular Discovery and Evaluation Facility for the establishment of xenograft tumors, blood collections, and animal cares. This work was supported, in part, by grants from the U.S. Army Medical Research Acquisition Activity, Prostate Cancer Research Program grant PC073098, Purdue University Center for Cancer Research Small Grants Program, and the Indian Clinical and Translational Science Institute funded, in part, by RR025761 from the National Institutes of Health, National Center for Research Resources, Clinical and Translational Sciences Award. DNA sequencing and animal experiments were conducted in the Purdue University Center for Cancer Research Genomic Core Facility and the Molecular Discovery and Evaluation Facility supported by NCI CCSG CA23168 to Purdue University Center for Cancer Research.

References

[1] Jemal A, Siegel R, Ward E, Hao Y, Xu J and Thun MJ. Cancer statistics, 2009. CA Cancer J Clin 2009;59:225-49.

[2] Kuban DA, Thames HD, Levy LB, Horwitz EM, Kupelian PA, Martinez AA, Michalski JM, Pisansky TM, Sandler HM, Shipley WU, Zelefsky MJ and Zietman AL. Long-term multi-institutional analysis of stage T1-T2 prostate cancer treated with radiotherapy in the PSA era. Int J Radiat Oncol Biol Phys 2003;57:915-28.

[3] Zietman AL, DeSilvio ML, Slater JD, Rossi CJ, Jr., Miller DW, Adams JA and Shipley WU. Comparison of conventional-dose vs high-dose conformal radiation therapy in clinically localized adenocarcinoma of the prostate: a randomized controlled trial. JAMA 2005;294:1233-9.

[4] D'Amico AV, Chen MH, Renshaw AA, Loffredo B and Kantoff PW. Risk of prostate cancer recurrence in men treated with radiation alone or in conjunction with combined or less than combined androgen suppression therapy. J Clin Oncol 2008;26:2979-83.

[5] Agarwal PK, Sadetsky N, Konety BR, Resnick MI and Carroll PR. Treatment failure after primary and salvage therapy for prostate cancer: likelihood, patterns of care, and outcomes. Cancer 2008;112:307-14.

[6] Kimura M, Mouraviev V, Tsivian M, Mayes JM, Satoh T and Polascik TJ. Current salvage methods for recurrent prostate cancer after failure of primary radiotherapy. BJU Int 2009;

[7] Raldow A, Hamstra DA, Kim SN and Yu JB. Adjuvant radiotherapy after radical prostatectomy: evidence and analysis. Cancer Treat Rev 2011;37:89-96.

[8] Rosenthal SA and Sandler HM. Treatment strategies for high-risk locally advanced prostate cancer. Nat Rev Urol 2010;7:31-8.

[9] Choe KS and Liauw SL. Radiotherapeutic strategies in the management of low-risk prostate cancer. ScientificWorldJournal 2010;10:1854-69.

[10] Cooperberg MR, Broering JM, Litwin MS, Lubeck DP, Mehta SS, Henning JM and Carroll PR. The contemporary management of prostate cancer in the United States: lessons from the cancer of the prostate strategic urologic research endeavor (CapSURE), a national disease registry. J Urol 2004;171:1393-401.

[11] Trock BJ, Han M, Freedland SJ, Humphreys EB, DeWeese TL, Partin AW and Walsh PC. Prostate cancer-specific survival following salvage radiotherapy vs observation in men with biochemical recurrence after radical prostatectomy. JAMA 2008;299:2760-9.

[12] Chin JL. Post-radical prostatectomy management options for the positive surgical margin: argument for adjuvant radiotherapy. Urol Oncol 2009;27:87-8.

[13] Bolla M, Van Tienhoven G, Warde P, Dubois JB, Mirimanoff RO, Storme G, Bernier J, Kuten A, Sternberg C, Billiet I, Torecilla JL, Pfeffer R, Cutajar CL, Van der Kwast T and Collette L. External irradiation with or without long-term androgen suppression for prostate cancer with high metastatic risk: 10-year results of an EORTC randomised study. Lancet Oncol 2010;11:1066-73.

[14] Daneshmand S, Quek ML and Pinski J. Neuroendocrine differentiation in prostate cancer. Cancer Therapy 2005;3:383-396.

[15] Nelson EC, Cambio AJ, Yang JC, Ok JH, Lara PN, Jr. and Evans CP. Clinical implications of neuroendocrine differentiation in prostate cancer. Prostate Cancer Prostatic Dis 2007;10:6-14.

[16] Bonkhoff H. Neuroendocrine differentiation in human prostate cancer. Morphogenesis, proliferation and androgen receptor status. Ann Oncol 2001;12 Suppl 2:S141-4.

[17] Amorino GP and Parsons SJ. Neuroendocrine cells in prostate cancer. Crit Rev Eukaryot Gene Expr 2004;14:287-300.

[18] Cox ME, Deeble PD, Lakhani S and Parsons SJ. Acquisition of neuroendocrine characteristics by prostate tumor cells is reversible: implications for prostate cancer progression. Cancer Res 1999;59:3821-30.
[19] Deng X, Liu H, Huang J, Cheng L, Keller ET, Parsons SJ and Hu CD. Ionizing radiation induces prostate cancer neuroendocrine differentiation through interplay of CREB and ATF2: Implications for disease progression. Cancer Res. 2008;68:9663-9670.
[20] Wang JC. Finding primary targets of transcriptional regulators. Cell Cycle 2005;4:356-8.
[21] Humez S, Monet M, Legrand G, Lepage G, Delcourt P and Prevarskaya N. Epidermal growth factor-induced neuroendocrine differentiation and apoptotic resistance of androgen-independent human prostate cancer cells. Endocr Relat Cancer 2006;13:181-95.
[22] Huang J, Wu C, di Sant'Agnese PA, Yao JL, Cheng L and Na Y. Function and molecular mechanisms of neuroendocrine cells in prostate cancer. Anal Quant Cytol Histol 2007;29:128-38.
[23] Zelivianski S, Verni M, Moore C, Kondrikov D, Taylor R and Lin MF. Multipathways for transdifferentiation of human prostate cancer cells into neuroendocrine-like phenotype. Biochim Biophys Acta 2001;1539:28-43.
[24] di Sant'Agnese PA. Neuroendocrine differentiation in prostatic carcinoma: an update on recent developments. Ann Oncol 2001;12 Suppl 2:S135-40.
[25] Komiya A, Suzuki H, Imamoto T, Kamiya N, Nihei N, Naya Y, Ichikawa T and Fuse H. Neuroendocrine differentiation in the progression of prostate cancer. Int J Urol 2009;16:37-44.
[26] Kamiya N, Suzuki H, Kawamura K, Imamoto T, Naya Y, Tochigi N, Kakuta Y, Yamaguchi K, Ishikura H and Ichikawa T. Neuroendocrine differentiation in stage D2 prostate cancers. Int J Urol 2008;15:423-8.
[27] Berruti A, Mosca A, Porpiglia F, Bollito E, Tucci M, Vana F, Cracco C, Torta M, Russo L, Cappia S, Saini A, Angeli A, Papotti M, Scarpa RM and Dogliotti L. Chromogranin A expression in patients with hormone naive prostate cancer predicts the development of hormone refractory disease. J Urol 2007;178:838-43; quiz 1129.
[28] Angelsen A, Syversen U, Haugen OA, Stridsberg M, Mjolnerod OK and Waldum HL. Neuroendocrine differentiation in carcinomas of the prostate: do neuroendocrine serum markers reflect immunohistochemical findings? Prostate 1997;30:1-6.
[29] Berruti A, Dogliotti L, Mosca A, Bellina M, Mari M, Torta M, Tarabuzzi R, Bollito E, Fontana D and Angeli A. Circulating neuroendocrine markers in patients with prostate carcinoma. Cancer 2000;88:2590-7.
[30] Taplin ME, George DJ, Halabi S, Sanford B, Febbo PG, Hennessy KT, Mihos CG, Vogelzang NJ, Small EJ and Kantoff PW. Prognostic significance of plasma chromogranin a levels in patients with hormone-refractory prostate cancer treated in Cancer and Leukemia Group B 9480 study. Urology 2005;66:386-91.
[31] Sciarra A, Monti S, Gentile V, Mariotti G, Cardi A, Voria G, Lucera R and Di Silverio F. Variation in chromogranin A serum levels during intermittent versus continuous androgen deprivation therapy for prostate adenocarcinoma. Prostate 2003;55:168-79.
[32] Sasaki T, Komiya A, Suzuki H, Shimbo M, Ueda T, Akakura K and Ichikawa T. Changes in chromogranin a serum levels during endocrine therapy in metastatic prostate cancer patients. Eur Urol 2005;48:224-9; discussion 229-30.
[33] Vashchenko N and Abrahamsson PA. Neuroendocrine differentiation in prostate cancer: implications for new treatment modalities. Eur Urol 2005;47:147-55.
[34] Bang YJ, Pirnia F, Fang WG, Kang WK, Sartor O, Whitesell L, Ha MJ, Tsokos M, Sheahan MD, Nguyen P and et al. Terminal neuroendocrine differentiation of human prostate carcinoma cells in response to increased intracellular cyclic AMP. Proc Natl Acad Sci U S A 1994;91:5330-4.

[35] Farini D, Puglianiello A, Mammi C, Siracusa G and Moretti C. Dual effect of pituitary adenylate cyclase activating polypeptide on prostate tumor LNCaP cells: short- and long-term exposure affect proliferation and neuroendocrine differentiation. Endocrinology 2003;144:1631-43.
[36] Deeble PD, Murphy DJ, Parsons SJ and Cox ME. Interleukin-6- and cyclic AMP-mediated signaling potentiates neuroendocrine differentiation of LNCaP prostate tumor cells. Mol Cell Biol 2001;21:8471-82.
[37] Lee SO, Chun JY, Nadiminty N, Lou W and Gao AC. Interleukin-6 undergoes transition from growth inhibitor associated with neuroendocrine differentiation to stimulator accompanied by androgen receptor activation during LNCaP prostate cancer cell progression. Prostate 2007;67:764-73.
[38] Qiu Y, Robinson D, Pretlow TG and Kung HJ. Etk/Bmx, a tyrosine kinase with a pleckstrin-homology domain, is an effector of phosphatidylinositol 3'-kinase and is involved in interleukin 6-induced neuroendocrine differentiation of prostate cancer cells. Proc Natl Acad Sci U S A 1998;95:3644-9.
[39] Spiotto MT and Chung TD. STAT3 mediates IL-6-induced neuroendocrine differentiation in prostate cancer cells. Prostate 2000;42:186-95.
[40] Wang Q, Horiatis D and Pinski J. Inhibitory effect of IL-6-induced neuroendocrine cells on prostate cancer cell proliferation. Prostate 2004;61:253-9.
[41] Wang Q, Horiatis D and Pinski J. Interleukin-6 inhibits the growth of prostate cancer xenografts in mice by the process of neuroendocrine differentiation. Int J Cancer 2004;111:508-13.
[42] Xie S, Lin HK, Ni J, Yang L, Wang L, di Sant'Agnese PA and Chang C. Regulation of interleukin-6-mediated PI3K activation and neuroendocrine differentiation by androgen signaling in prostate cancer LNCaP cells. Prostate 2004;60:61-7.
[43] Ismail AH, Landry F, Aprikian AG and Chevalier S. Androgen ablation promotes neuroendocrine cell differentiation in dog and human prostate. Prostate 2002;51:117-25.
[44] Jiborn T, Bjartell A and Abrahamsson PA. Neuroendocrine differentiation in prostatic carcinoma during hormonal treatment. Urology 1998;51:585-9.
[45] Jin RJ, Wang Y, Masumori N, Ishii K, Tsukamoto T, Shappell SB, Hayward SW, Kasper S and Matusik RJ. NE-10 neuroendocrine cancer promotes the LNCaP xenograft growth in castrated mice. Cancer Res 2004;64:5489-95.
[46] Wright ME, Tsai MJ and Aebersold R. Androgen receptor represses the neuroendocrine transdifferentiation process in prostate cancer cells. Mol Endocrinol 2003;17:1726-37.
[47] Yuan TC, Veeramani S, Lin FF, Kondrikou D, Zelivianski S, Igawa T, Karan D, Batra SK and Lin MF. Androgen deprivation induces human prostate epithelial neuroendocrine differentiation of androgen-sensitive LNCaP cells. Endocr Relat Cancer 2006;13:151-67.
[48] Zhang XQ, Kondrikov D, Yuan TC, Lin FF, Hansen J and Lin MF. Receptor protein tyrosine phosphatase alpha signaling is involved in androgen depletion-induced neuroendocrine differentiation of androgen-sensitive LNCaP human prostate cancer cells. Oncogene 2003;22:6704-16.
[49] Sobel RE and Sadar MD. Cell lines used in prostate cancer research: a compendium of old and new lines--part 1. J Urol 2005;173:342-59.
[50] Lilleby W, Paus E, Skovlund E and Fossa SD. Prognostic value of neuroendocrine serum markers and PSA in irradiated patients with pN0 localized prostate cancer. Prostate 2001;46:126-33.
[51] Deeble PD, Cox ME, Frierson HF, Jr., Sikes RA, Palmer JB, Davidson RJ, Casarez EV, Amorino GP and Parsons SJ. Androgen-independent growth and tumorigenesis of prostate cancer cells are enhanced by the presence of PKA-differentiated neuroendocrine cells. Cancer Res 2007;67:3663-72.

[52] Rokhlin OW, Taghiyev AF, Bayer KU, Bumcrot D, Koteliansk VE, Glover RA and Cohen MB. Calcium/calmodulin-dependent kinase II plays an important role in prostate cancer cell survival. Cancer Biol Ther 2007;6:732-42.
[53] Mamaeva OA, Kim J, Feng G and McDonald JM. Calcium/calmodulin-dependent kinase II regulates notch-1 signaling in prostate cancer cells. J Cell Biochem 2009;106:25-32.
[54] Merkle D and Hoffmann R. Roles of cAMP and cAMP-dependent protein kinase in the progression of prostate cancer: cross-talk with the androgen receptor. Cell Signal 2011;23:507-15.
[55] Hensley HH, Hannoun-Levi JM, Hachem P, Mu Z, Stoyanova R, Khor LY, Agrawal S and Pollack A. PKA knockdown enhances cell killing in response to radiation and androgen deprivation. Int J Cancer 2011;128:962-73.
[56] Rokhlin OW, Guseva NV, Taghiyev AF, Glover RA and Cohen MB. KN-93 inhibits androgen receptor activity and induces cell death irrespective of p53 and Akt status in prostate cancer. Cancer Biol Ther 2010;9:224-35.
[57] Johannessen M and Moens U. Multisite phosphorylation of the cAMP response element-binding protein (CREB) by a diversity of protein kinases. Front Biosci 2007;12:1814-32.
[58] Dent P, Yacoub A, Contessa J, Caron R, Amorino G, Valerie K, Hagan MP, Grant S and Schmidt-Ullrich R. Stress and radiation-induced activation of multiple intracellular signaling pathways. Radiation Research 2003;159:283-300.
[59] Dent P, Yacoub A, Fisher PB, Hagan MP and Grant S. MAPK pathways in radiation responses. Oncogene 2003;22:5885-96.

Legends to Figures

Figure 1. IR induces NED in prostate cancer cells. A). Shown are representative images acquired from the indicated prostate cancer cells that were treated with 40 Gy of fractionated IR (IR+) or without IR treatment (IR-). **B).** Cells were harvested from experiments in A and approximately 40 μg of total lysate was used for immunoblotting analysis of CgA, NSE and β-Actin. Similar results were reproduced from at least three independent experiments.

Figure 2: IR induces CREB activation and cytoplasmi sequestration of ATF2 in prostate cancer cells. A). Shown is a representative immunoblotting analysis of phosphorylated CREB (pCREB) from non-irradiated cells (IR-) or from cells that received 10 Gy of fractionated IR (IR+). **B)**. Shown are DIC and fluorescent images for ATF2 or DNA (DAPI) acquired from the indicated non-irradiated prostate cancer cells (IR-) or from cells that received 10 Gy of fractionated IR (IR+). These experiments were reproduced for at least three times and similar results were obtained.

Figure 3: Activated CREB induces neurite outgrowth and the expression of CgA and NSE in PC-3 and DU-145 cells. **A)**. Prostate cancer cells PC-3 and DU-145 were transfected with a pHA-CMV plasmid encoding a constitutively activated CREB, VP16-bCREB (bCREB), or the pHA-CMV empty vector (Vec). Shown are phase contrast images acquired five days after the transfection. **B)** and **C)**. Expression of HA-VP16-bCREB (HA), CgA, NSE and β-Actin in PC-3 cells (B) or DU-145 cells (C) from the experiments in A. Note that CgA was not detectable in PC-3 cells transfected with the vector control pHA-CMV or pHA-VP16-bCREB.

Figure 4: ATF2 knockdown induces neurite outgrowth and the expression of CgA and NSE in prostate cancer cells. A). Prostate cancer cells PC-3 and DU-145 were transfected with the ATF2 shRNA plasmid (ATF2 KD) or the scrambled control (SC). Shown are phase contrast

images acquired five days after the transfection. **B)** and **C)**. Expression of ATF2, CgA, NSE and β-Actin in PC-3 cells (B) or DU-145 cells (C) from the experiments in A. Note that CgA was not detectable in PC-3 cells transfected with either SC or ATF2 shRNA plasmids.

Figure 5. Ionizing radiation induces CgA expression in prostate cancer xenograft tumors and an increase of plasma CgA levels in nude mice. **A)**. IHC analysis of CgA expression in irradiated LNCaP xenograft tumors after 40 Gy of irradiation (IR+) or in non-irradiated xenograft tumors. **B)**. Average fold change of plasma CgA levels normalized to plasma PSA at the end of week 2 and week 4 when compared with those before irradiation (0). Similar time points were followed for blood collection from tumor-bearing mice that did not receive radiation treatment. The average fold change presented is from all 10 mice for each group.

Figure 6. Radiotherapy increases serum CgA levels in prostate cancer patients. All 9 prostate cancer patients were diagnosed with localized tumors and treated at the Midwest Proton Radiotherapy Instituted with 72 Gy (2 Gy/fraction). Blood samples were collected before the treatment (Before), in the middle of RT (Middle) and after RT (After). The serum CgA levels were normalized to the serum PSA levels, and the fold change at Middle and After time points is presented for each patient.

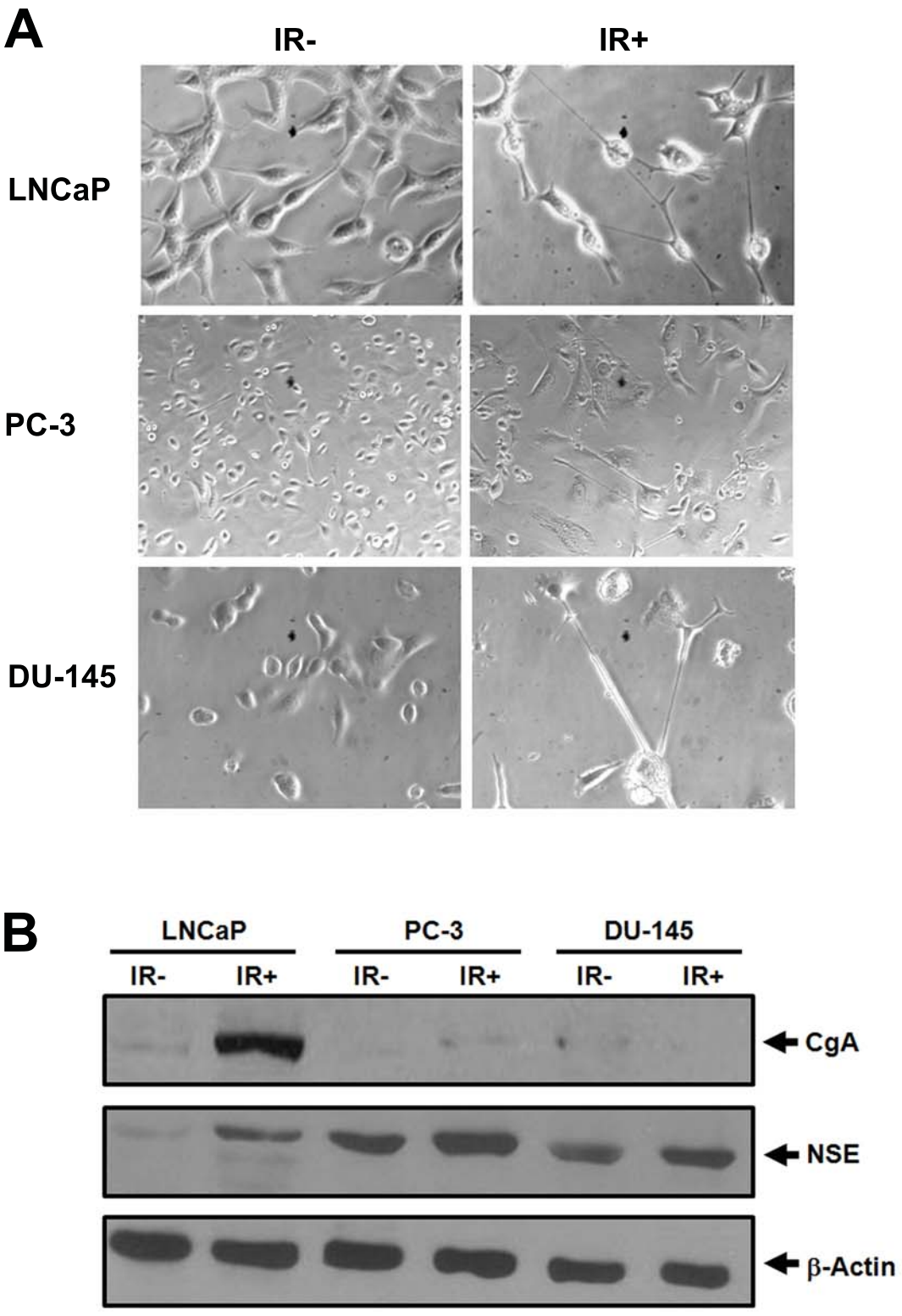
A
IR-
IR+
LNCaP
PC-3
DU-145
B
LNCaP
PC-3
DU-145
IR-
IR+
IR-
IR+
IR-
IR+
CgA
NSE
β-Actin

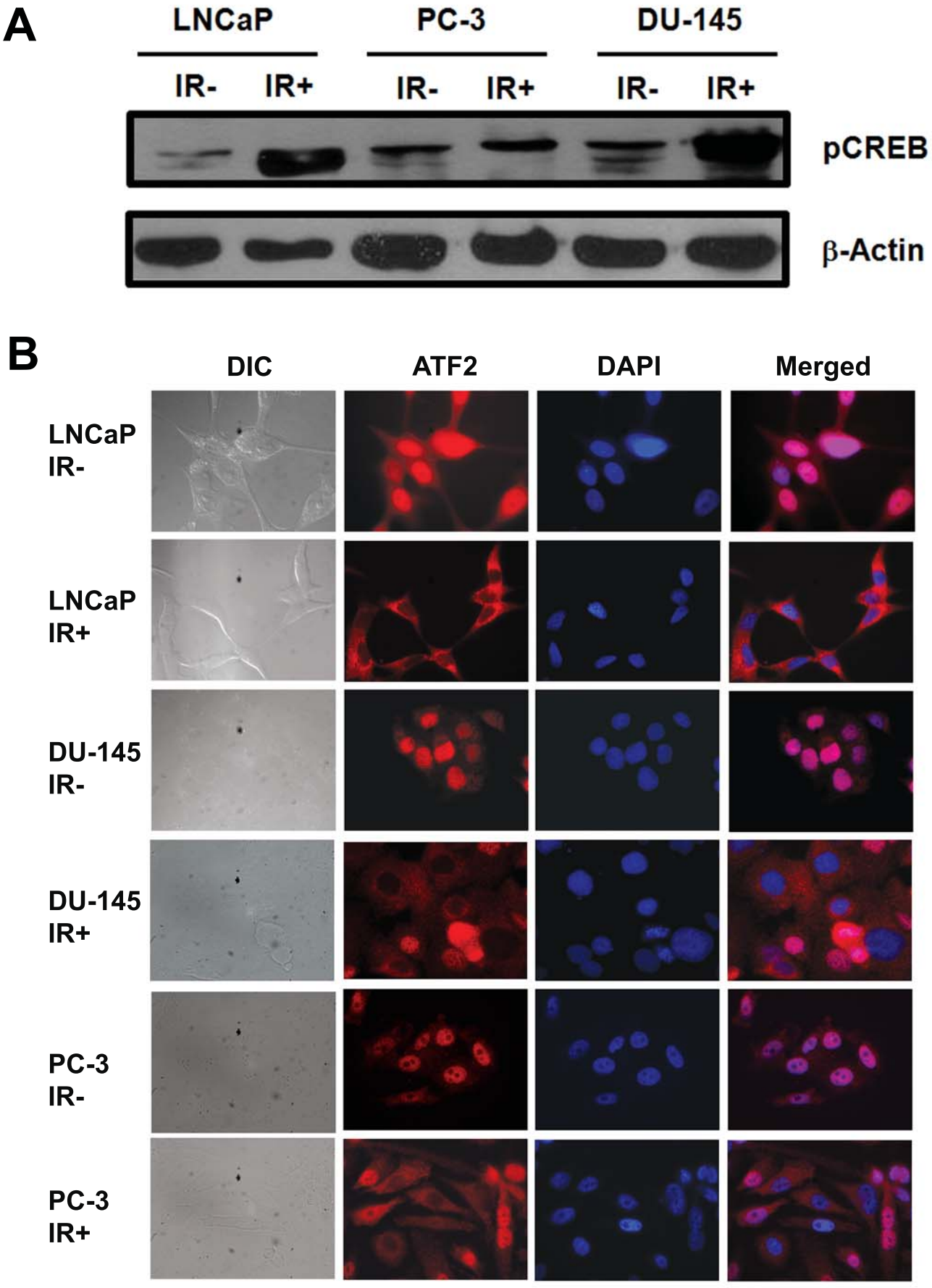
A
LNCaP
PC-3
DU-145
IR-
IR+
IR-
IR+
IR-
IR+
pCREB
β-Actin
B
DIC
ATF2
DAPI
Merged
LNCaP IR-
LNCaP IR+
DU-145 IR-
DU-145 IR+
PC-3 IR-
PC-3 IR+

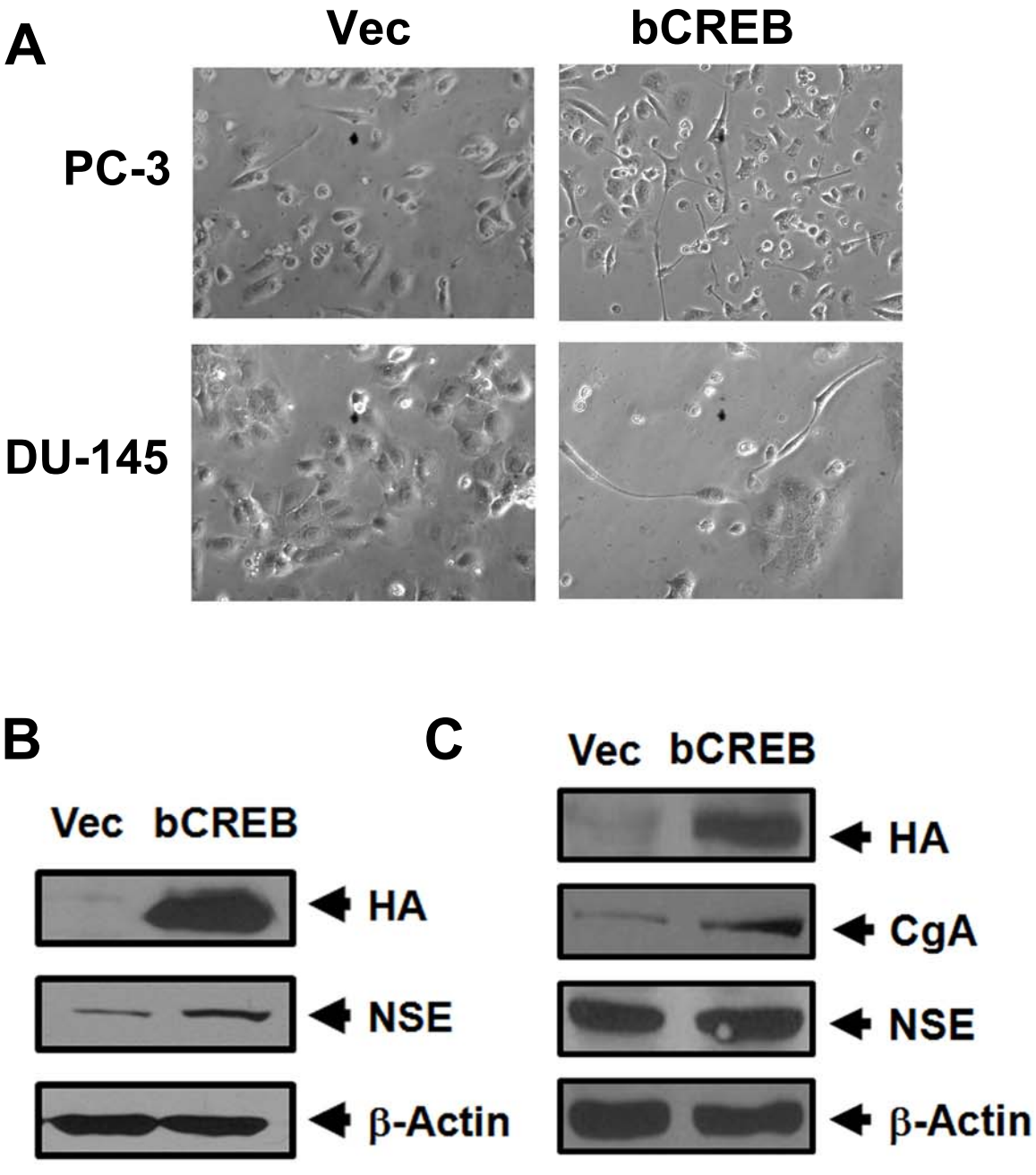
A
Vec
bCREB
PC-3
DU-145
B
Vec bCREB
HA
NSE
β-Actin
C
Vec bCREB
HA
CgA
NSE
β-Actin

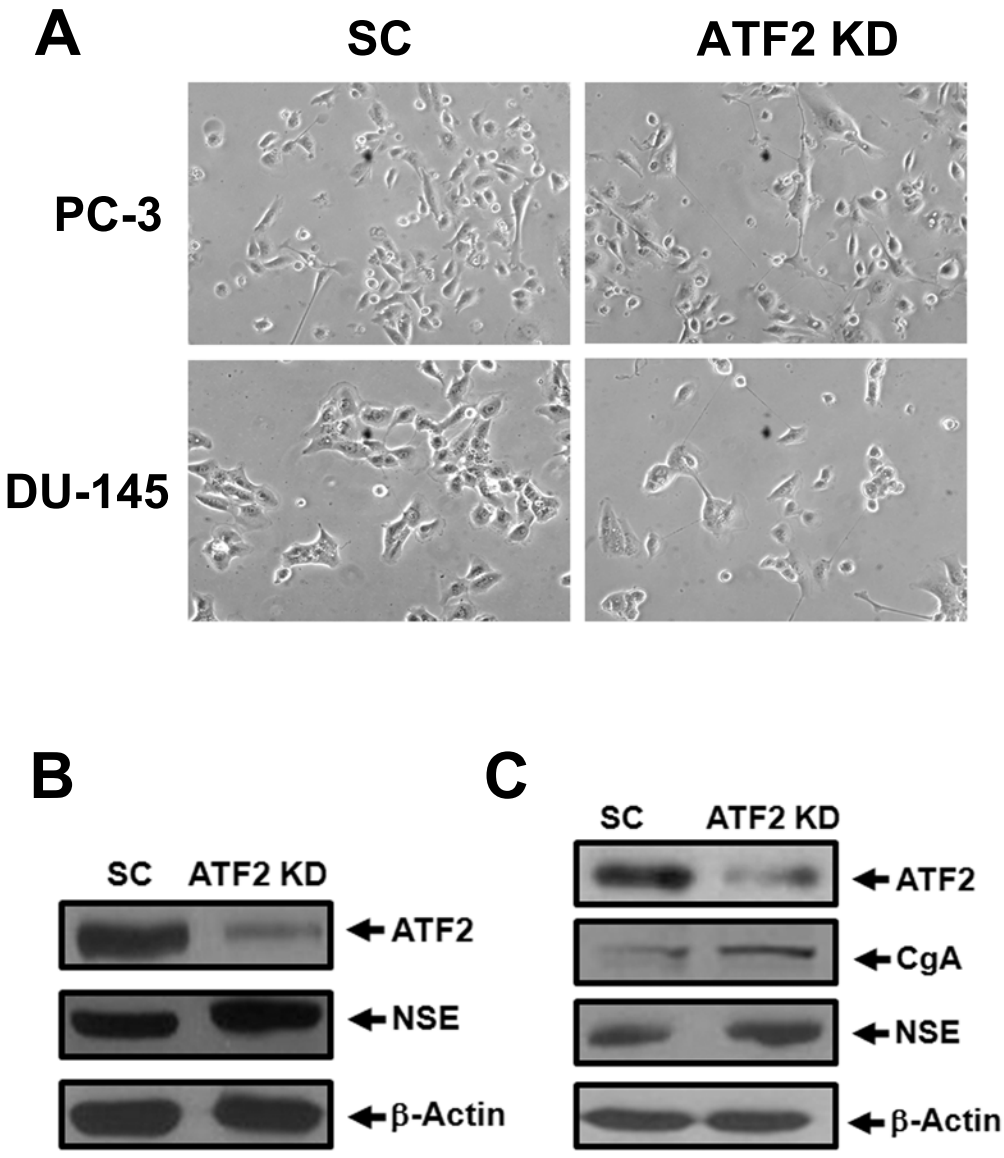
A
SC
ATF2 KD
PC-3
DU-145
B
SC
ATF2 KD
ATF2
NSE
β-Actin
C
SC
ATF2 KD
ATF2
CgA
NSE
β-Actin

Deng et al., Figure 5

A

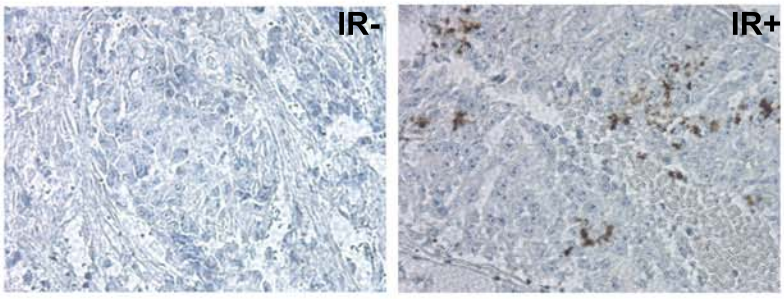

B

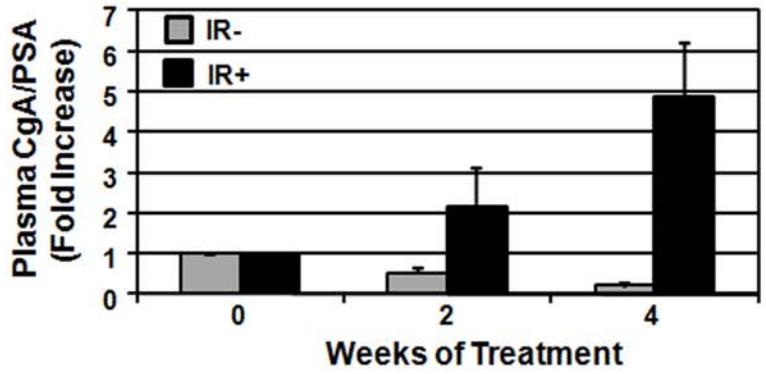

Deng et al., Figure 6

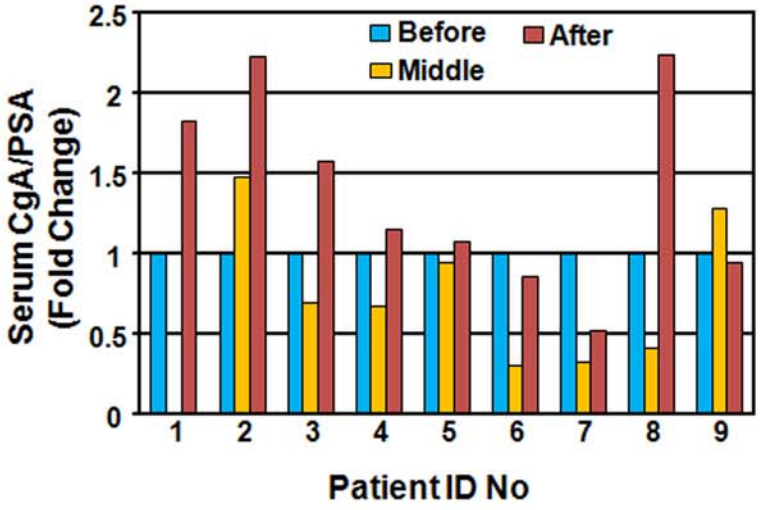

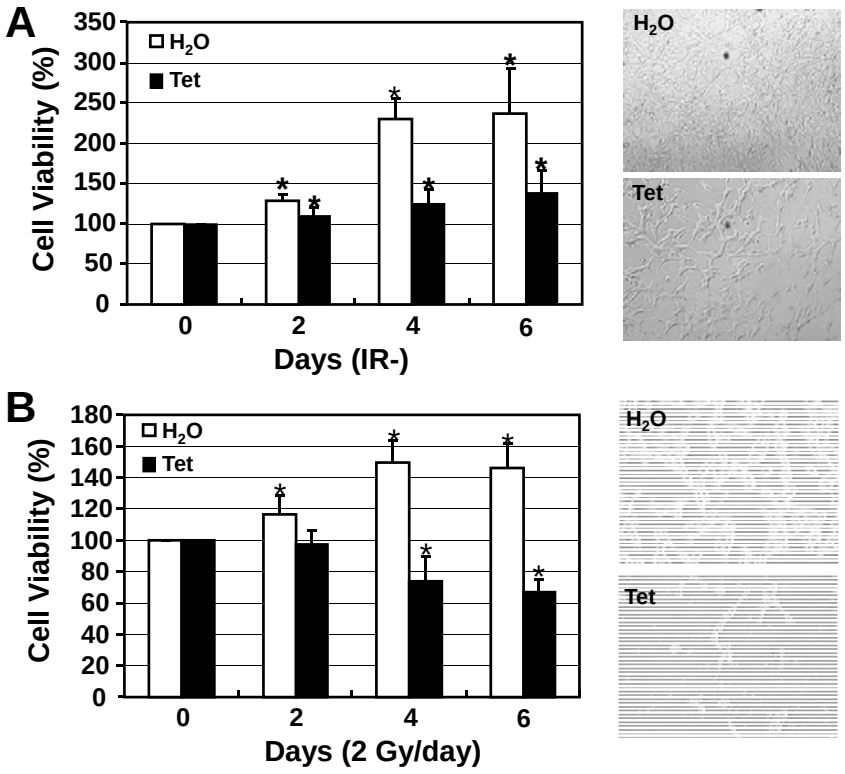

Figure 1. CREB targeting sensitizes prostate cancer cells to radiation. A. A representative stable cell line was seeded in 48-well plates and induced to express A-CREB by tetracycline (Tet) or without A-CREB induction (H_2O). Cell viability was assayed using the MTT assay at the indicated days. Right panels show cell images after 10 Gy of irradiation. **B**. Similar experiments were performed in A except that cells were subjected to fractionated IR (2 Gy/day) starting from Day 0. * $p<0.01$ when compared with Day 0.

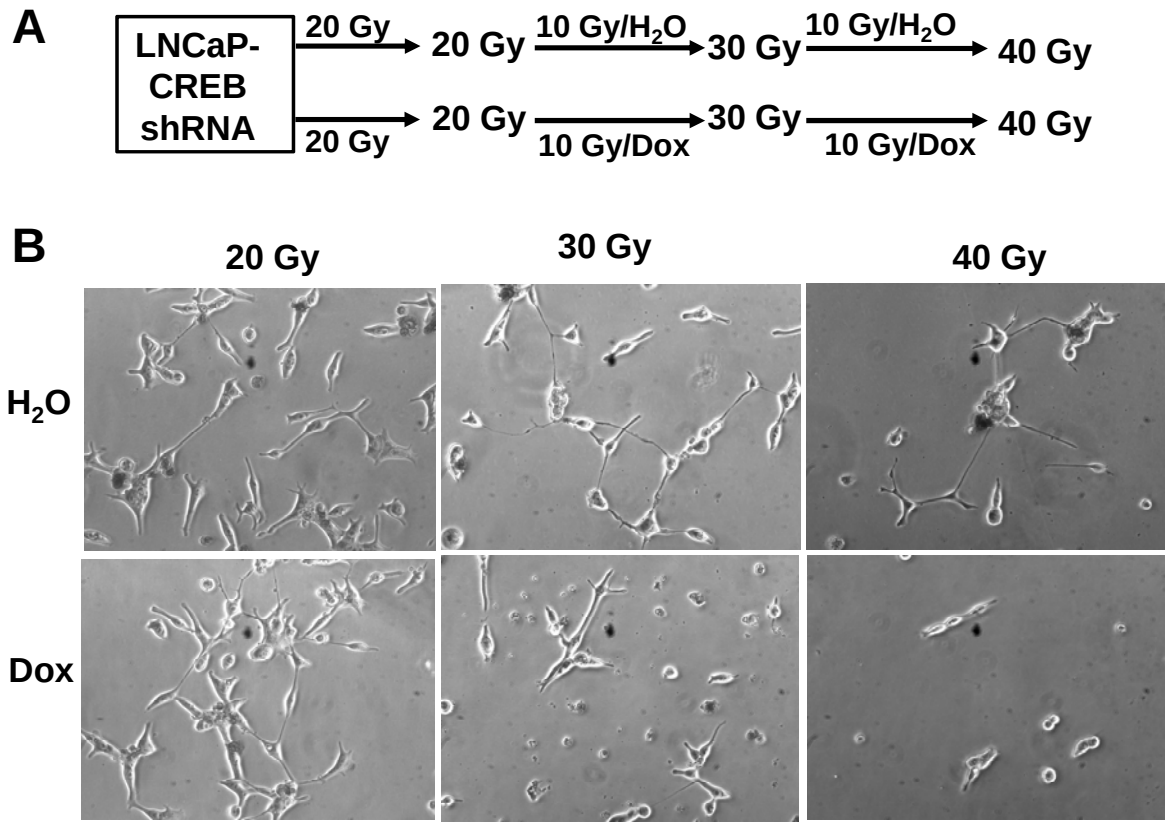

Figure 2. Inhibition of IR-induced NED per se is sufficient to sensitize prostate cancer cells to radiation. A. Show is the scheme of treatments of LNCaP stable cell lines that can inducibly express CREB shRNA. Cells were first irradiated for two weeks (20 Gy) without the induction of CREB shRNA by doxycline (Dox). Beginning the third week, cells were treated with Dox to induce CREB shRNA expression. The control group was treated with H_2O only. Cells were continued irradiated and treatment for the third (30 Gy) and fourth week (40 Gy). **B.** Shown are representative images of cells that were irradiated for 20 Gy, 30 Gy and 40 Gy with or without the induction of CREB shRNA during the third and fourth week treatment.

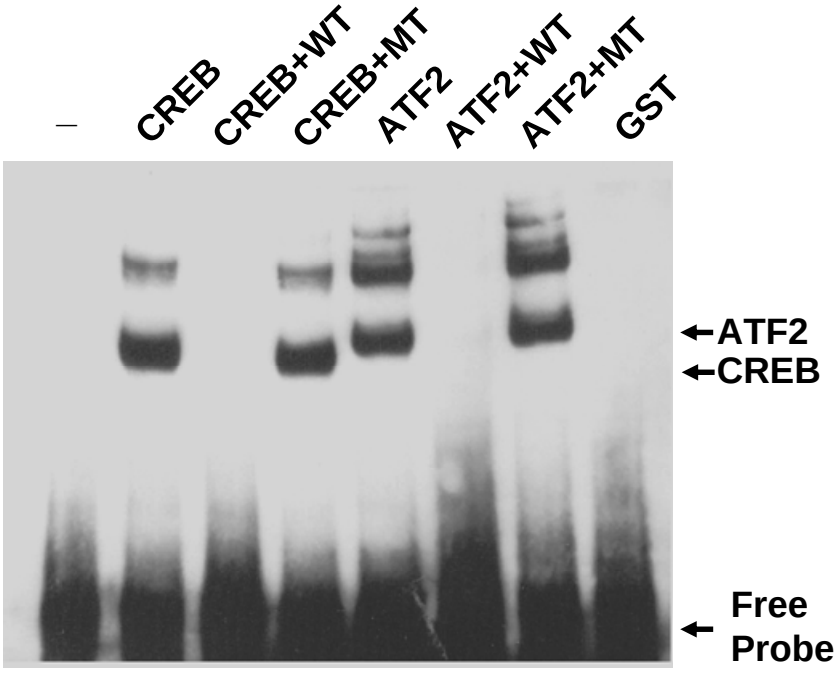

Figure 3. DNA binding of ATF2 and CREB to CgA. The bZIP regions of CREB and ATF2 were expressed in *E. coli* and purified as GST-tagged fusion proteins. Approximately 2 pmol of indicated purified fusion proteins were incubated with 50 ng of biotin-labeled CRE consensus sequences derived from the CgA promoter in the absence or presence of 100x unlabeled wild-type (WT) or mutant (MT) probes. The protein-DNA complexes were resolved on a 4% polyacrylamide gel, transferred and crosslinked to Nylon membrane. The detection of protein-DNA complexes was performed by incubating the membrane with Streptavidin-HRP followed by ECL. The arrows indicate the positions of DNA-protein complexes composed of CREB homodimers or ATF2 homodimers. Note that one slower mobility shift band for both ATF2 and CREB likely represents oligomers bound to DNA, which are often seen with other bZIP proteins.

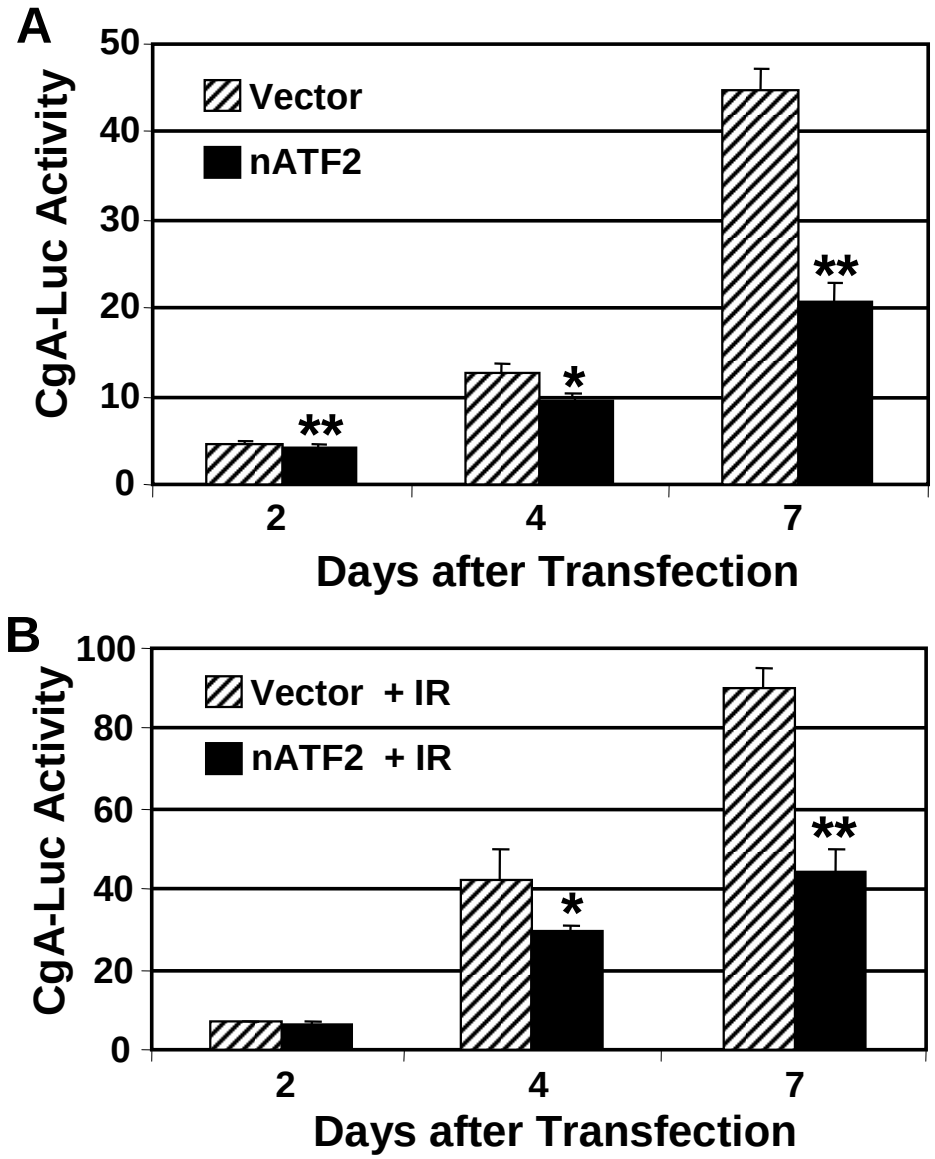

Figure 4: Inhibition of CgA-Luc reporter gene activity by nATF2 in LNCaP cells. LNCaP cells cultured in 12-well plates were co-transfected with 0.5 μg of the reporter plasmid pGL4.10-CgA-Luc and 50 ng of pRL-TK with 0.5 μg of the vector control (vector) or the plasmid encoding the constitutively nuclear-localized ATF2 (nATF2) using FuGENE HD. The transfected cells were left untreated (**A**) or irradiated every day (2 Gy/day) (**B**), and harvested at the indicated time posttransfection. Five μg of total protein was used for the measurement of luciferase activity using the Dual-Luciferasce Assay kit (Promega). *$p<0.05$ when compared with the respective vector control. **$p<0.01$ when compared with the respective vector control.

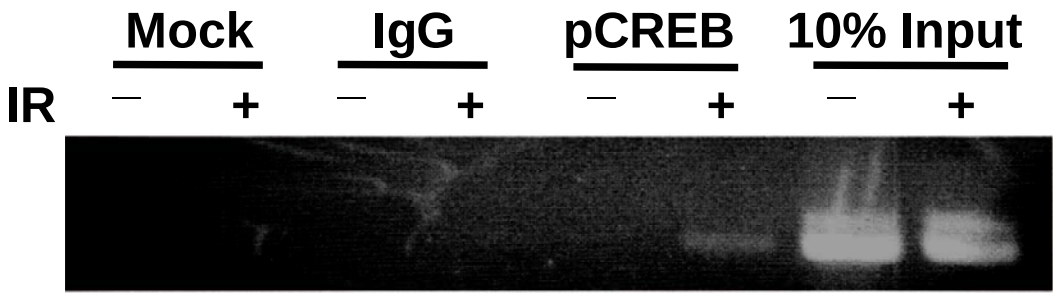

Figure 5. ChIP analysis of pCREB binding to the CgA promoter in LNCaP cells. DNA-protein complexes in non-irradaited (IR-) or irradiated for five times (IR+) LNCaP cells were crosslinked in whole cells using formaldehyde. Following nuclei isolation and lysis, the chromatin was sonicated to an average length of ~600 bp prior to immunoprecipitation with the antibody against phospho-CREB and mouse IgG (IgG) or without antibody (Mock). The proteins in the immunoprecipitates were digested by Protease K and the DNA was directly extracted using Chelex beads. The DNA eluted from the beads was used for PCR

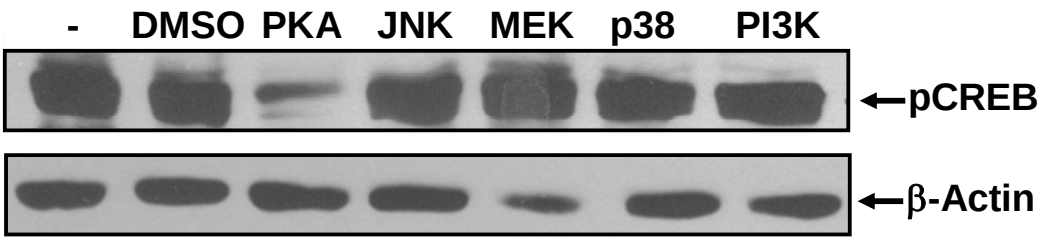

Figure 6. PKA mediates IR-induced CREB phosphorylation. LNCaP cells cultured in 10-cm dishes were irradiated (2 Gy/day) for five days in the absence (DMSO) or presence of the indicated protein kinase inhibitors at the commonly used concentrations. Total cell lysate was prepared after the treatment and subjected to immunoblotting analysis of pCREB. The lack of effect of an AKT inhibitor on IR-induced CREB phosphorylation was performed in a different experiment and was not included here.

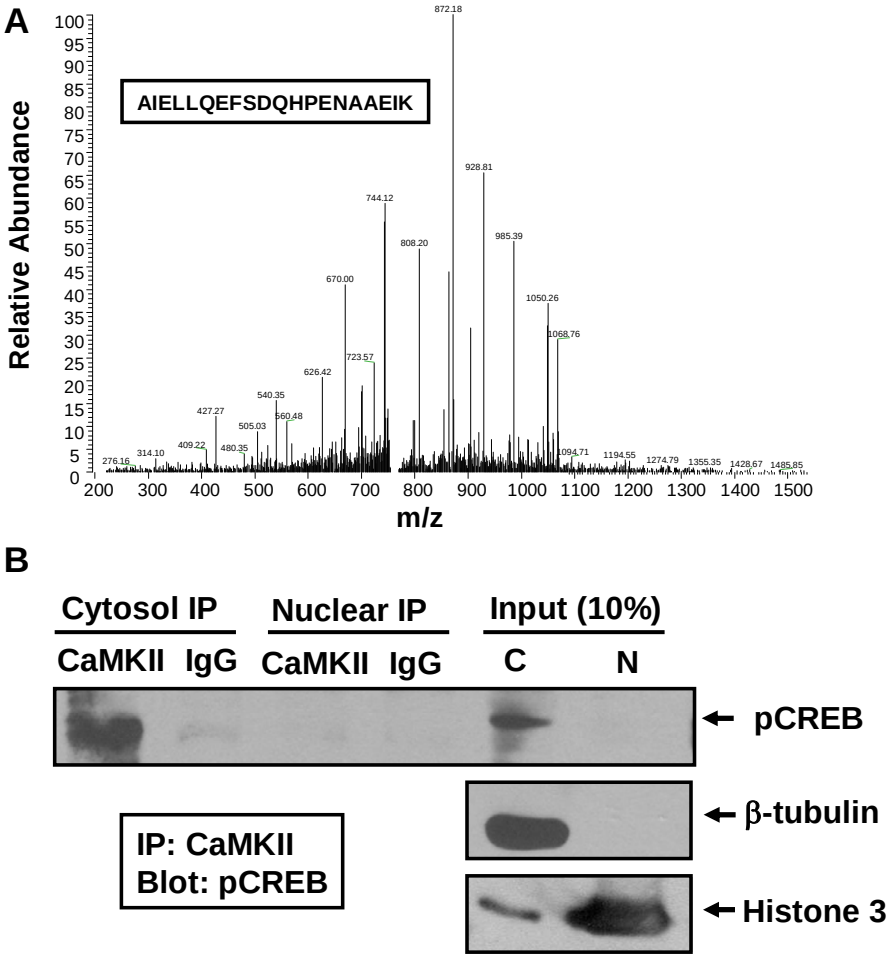

Figure 7. CaMKII interacts with pCREB in LNCaP cells. A. LNCaP cells were cultured to confluence and cytosolic extract was prepared. Approximately 1 mg of cytosolic extract was used to immunoprecipitate CREB with anti-CREB antibody and the immunoprecipitate was processed for mass spectrometry analysis. Shown is the spectrum for one of the peptides indentified. The insert shows the peptide sequence. **B**. Cytosolic extract (1 mg) and equal portion of nuclear extract from non-irradiated cells were used to immunoprecipitate CaMKII and blotted for pCREB. The input (10%) for both cytosolic (C) and nuclear (N) fractions was loaded on the last two lanes. Histone 3 and β-tubulin immunoblotting shown below were used as evidence of a successful fractionation.

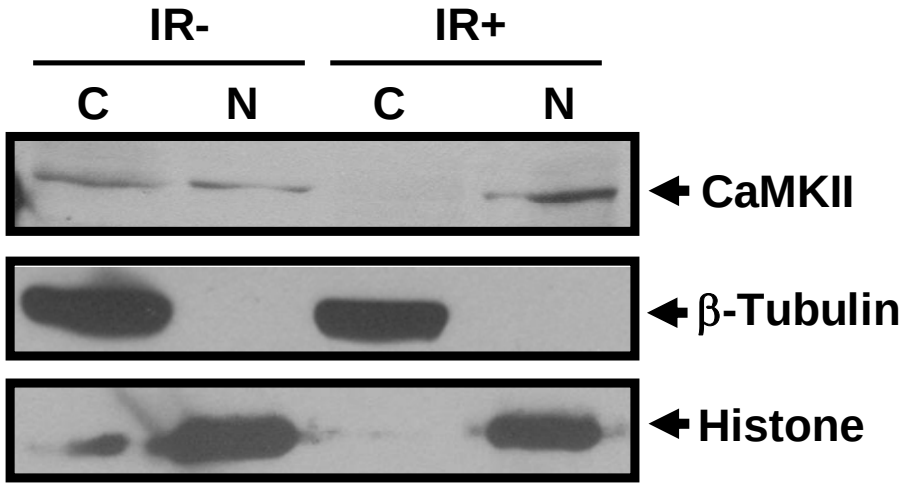

Figure 8. IR increases nuclear localization of CaMKII in LNCaP cells. LNCaP cells cultured in 10-cm dishes were irradiated for five days (2 Gy/day) (IR+) or without irradiation (IR-) and harvested for preparation of cytosolic and nuclear fractionations. Equal portion of cytosolic and nuclear fractions was subjected to immunoblotting analysis of CaMKII. Intensity-based quantification showed that 41% of total CaMKII was located in the nucleus in non-irradiated cells whereas 81% in the nucleus in irradiated cells.